Dalton Transactions

An international journal of inorganic chemistry

www.rsc.org/dalton

Number 21 | 7 June 2008 | Pages 2769–2900

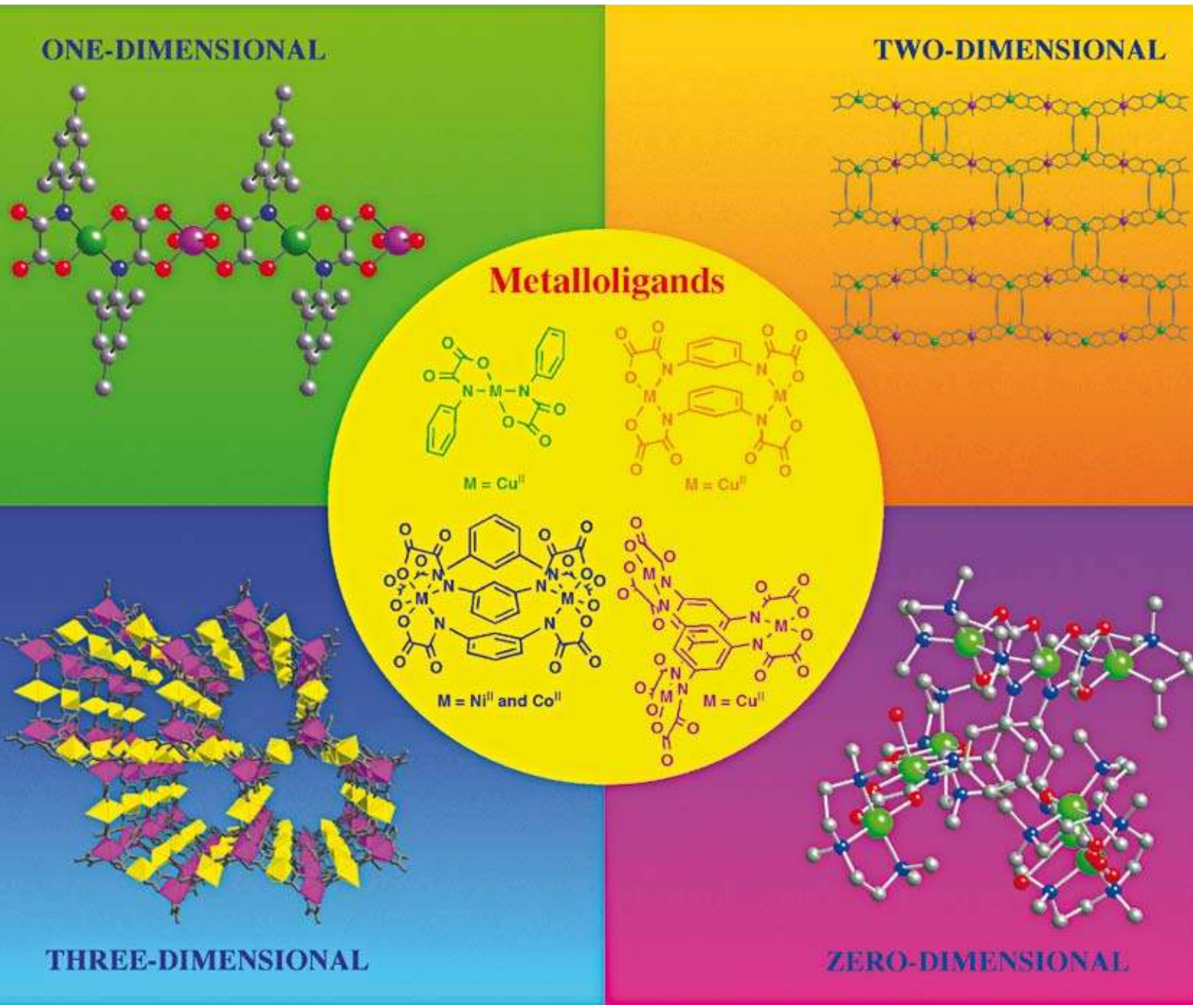

ISSN 1477-9226

RSC Publishing

Ligand design for multidimensional magnetic materials: a metallosupramolecular perspective

Emilio Pardo,[a] Rafael Ruiz-García,[b,c] Joan Cano,[d,e] Xavier Ottenwaelder,[f] Rodrigue Lescouëzec,[g] Yves Journaux,*[g] Francesc Lloret*[a] and Miguel Julve*[a]

Received 22nd January 2008, Accepted 25th February 2008
First published as an Advance Article on the web 10th April 2008
DOI: 10.1039/b801222a

The aim and scope of this review is to show the general validity of the 'complex-as-ligand' approach for the rational design of metallosupramolecular assemblies of increasing structural and magnetic complexity. This is illustrated herein on the basis of our recent studies on oxamato complexes with transition metal ions looking for the limits of the research avenue opened by Kahn's pioneering research twenty years ago. The use as building blocks of mono-, di- and trinuclear metal complexes with a novel family of aromatic polyoxamato ligands allowed us to move further in the coordination chemistry-based approach to high-nuclearity coordination compounds and high-dimensionality coordination polymers. In order to do so, we have taken advantage of the new developments of metallosupramolecular chemistry and in particular, of the molecular-programmed self-assembly methods that exploit the coordination preferences of metal ions and specifically tailored ligands. The judicious choice of the oxamato metal building block (substitution pattern and steric requirements of the bridging ligand, as well as the electronic configuration and magnetic anisotropy of the metal ion) allowed us to control the overall structure and magnetic properties of the final multidimensional *n*D products ($n = 0$–3). These species exhibit interesting magnetic properties which are brand-new targets in the field of molecular magnetism, such as single-molecule or single-chain magnets, and the well-known class of molecule-based magnets. This unique family of molecule-based magnetic materials expands on the reported examples of *n*D species with cyanide and related oxalato and dithiooxalato analogues. Moreover, the development of new oxamato metal building blocks with potential photo or redox activity at the aromatic ligand counterpart will provide us with addressable, multifunctional molecular materials for future applications in molecular electronics and nanotechnology.

Introduction: from molecular to supramolecular magnetism

Magnetism as a supramolecular function

Metallosupramolecular chemistry is an outstanding research area in the field of supramolecular chemistry.[1] Its spectacular development in the late eighties and nineties has set up the guiding principles for the self-assembly of well-defined multimetallic coordination architectures of increasing structural complexity based on metal–ligand interactions.[2] At the beginning of this new century, the introduction of functionality into these polymetallic systems has become one of the aims of a good number of research groups working in metallosupramolecular chemistry.[3–11] The study of the 'supramolecular structure–function' correlations will guide the rational design and synthesis of self-assembling functional metallosupramolecular complexes displaying interesting physico-chemical properties. They could be exploited in supramolecular research concerning electrochemistry,[11] photophysics,[5,6] molecule recognition and encapsulation,[4,5] and catalysis.[9]

Magnetism is a very good example of such a supramolecular function[12] in spite of being a relatively unexplored avenue in metallosupramolecular chemistry.[10,11] The magnetic properties of polymetallic systems derive from the cooperative exchange interactions between the paramagnetic metal ions through the bridging ligands. They therefore depend on the intrinsic nature of the individual metal and ligand constituents and the particular level of organization created by the metal–ligand coordinative interaction. In pursuing supramolecular magnetism, the ligand design is crucial both to organize the paramagnetic metal ions in a desired topology and to efficiently transmit exchange interactions between the metal ions in a controlled manner. This basic principle

[a]*Departament de Química Inorgànica, Instituto de Ciencia Molecular (ICMol), Universitat de València, Paterna, Valencia, Spain. E-mail: francisco.lloret@uv.es, miguel.julve@uv.es; Fax: +34 963544415; Tel: +34 963544442*
[b]*Departament de Química Orgànica, Instituto de Ciencia Molecular (ICMol), Universitat de València, Valencia, Spain*
[c]*Fundació General de la Universitat de València (FGUV), Universitat de València, Paterna, Valencia, Spain*
[d]*Departament de Química Inorgànica, Institut de Química Teòrica i Computacional (IQTC) and Institut de Nanociència i Nanotecnologia (IN2UB), Universitat de Barcelona, Barcelona, Spain*
[e]*Institució Catalana de Recerca i Estudis Avançats (ICREA), Universitat de Barcelona, Barcelona, Spain*
[f]*Department of Chemistry and Biochemistry, Concordia University, Montréal, Canada*
[g]*Laboratoire de Chimie Inorganique et Matériaux Moléculaires, UPMC Univ Paris 06, UMR, 7071, Paris, France. E-mail: jour@ccr.jussieu.fr; Fax: +33 144273841; Tel: +33 144275562*

Miguel Julve, Francesc Lloret and Yves Journaux

Dr Yves Journaux is the Director of the Inorganic Chemistry and Molecular Materials Laboratory in UPMC Université Paris 6, CNRS-associated laboratory (France), and Drs Francesc Lloret and Miguel Julve are Professors of Inorganic Chemistry at the University of Valencia (Spain). Their research activity focuses on coordination chemistry and molecular magnetism with special emphasis in the rational design of polynuclear complexes with predictable magnetic properties. The metal assembly and the magnetic interactions in these complexes are governed by varying the number and symmetry of the interacting magnetic orbitals and by playing on the nature of the blocking and bridging ligands. In recent years, they have paid special attention to the preparation, structural characterization and magnetic study of molecular nanomagnets.

is impressively demonstrated by the work on the magnetic properties of multimetallic coordination compounds build upon the classical cyanide (CN^-), oxalate and dithiooxalate ($C_2O_2X_2^{2-}$ with X = O and S) groups acting as bridging ligands.[13–19] These include both discrete, zero-dimensional (0D) high-nuclearity complexes as well as infinite, one- (1D), two- (2D), or three-dimensional (3D) polymers, also known as metal–organic coordination networks (MOCNs) or metal–organic frameworks (MOFs). These magnetically-coupled metallosupramolecular species whose dimensionality can be tuned will be of great importance in the so-called "bottom-up" approach to molecular magnetic materials, such as low-dimensional single-molecule (SMMs) and single-chain magnets (SCMs) and high-dimensional molecule-based magnets, with potential applications in information storage and processing nanotechnology.[20–22]

Since the early 1990s, the design and synthesis of high-dimensional 2D and 3D coordination polymers has been enhanced by the search of molecule-based compounds exhibiting a spontaneous magnetization below a critical temperature (T_C) greater than room temperature.[22] Indeed, long-range magnetic ordering is essentially a 3D phenomenon. There is no long-range magnetic ordering at a finite temperature for 1D systems; this is expected to occur at absolute zero for a chain in the lack of interchain interactions. However, long-range magnetic ordering may occur for a 2D system only if the magnetic anisotropy of the plane is of the Ising type. When compared with classical magnets based on metal oxides and metal alloys, these so-called molecule-based magnets show some advantageous physical properties such as transparency, lightness, and easy processability.

In the last few years, however, the search for low-dimensional 0D and 1D coordination polymers has became a priority in the field of molecular magnetism. This change of point of view has been motivated by the recent finding that these types of compounds could present a slow relaxation of the magnetization which is accompanied by magnetic hysteresis effects below a blocking temperature (T_B).[20,21] This unique magnetic behavior, which has no analogy in the world of classical magnetic materials, is not due to a long-range 3D magnetic order. In fact, it has a pure molecular origin which is associated with the peculiar magnetic anisotropy of either the polynuclear species or the chain. These new nanosized molecular magnetic materials, so-called SMMs and SCMs respectively, represent thus a chemical alternative to the "top-down" approach to multidispersed superparamagnetic nanoparticles of metal oxides and metal alloys.

Oxamato metal complexes in supramolecular magnetism

Oxamato-bridged polymetallic complexes deserve a particular attention in the young discipline of supramolecular magnetism because of the diversity of supramolecular architectures and magnetic properties that they can exhibit.[23] Discrete polynuclear coordination compounds as well as infinite multidimensional coordination polymers are included in this category.[24–27] The synthetic strategy for both families is based on the use of aliphatic and aromatic group-substituted oxamato-containing metal complexes as ligands toward other metal ions through the two *cis* carbonyl oxygen atoms of the oxamato groups (Scheme 1).[24]

There are well-known examples of the rational design of high-spin homo- and heterometallic polynuclear complexes which are based on the use of mono- and dinuclear oxamato copper(II) complexes as bis- or tetrakis(bidentate) ligands respectively, toward partially blocked metal complexes (Fig. 1).[25] Such an approach was initiated by Kahn and coworkers with the preparation of a series of oxamato-bridged $Cu^{II}M^{II}_2$ trimers (M = Cu, Ni, and Mn) from the copper(II) complex $[Cu(pba)]^{2-}$ [pba = *N*,*N*′-1,3-propylenebis(oxamate)] [Fig. 1(a)]. They exhibit S = 1/2 (M = Cu), 3/2 (M = Ni) and 9/2 (M = Mn) ground states as a result of the antiferromagnetic intratrimer coupling between the central Cu^{II} and the peripheral M^{II} ions through the oxamato bridge.[25a–c,e] It was then extended by Journaux and Aukauloo to a series of oxamato-bridged $Cu^{II}_2M^{II}_4$ hexamers (M = Cu and Ni) prepared from the ferromagnetically coupled dicopper(II) analogue $[Cu_2(bpba)]^{4-}$ [bpba = *N*,*N*′,*N*″,*N*‴-tetramethylenemethanetetrakis(oxamate)] [Fig. 1(b)], whereby the weak intramolecular ferromagnetic interaction between the central Cu^{II} ions through the tetramethylenemethanetetraamidate bridge would be masked by the intermolecular antiferromagnetic interactions and/or magnetic anisotropy effects.[25k] To our knowledge, however, no slow magnetic relaxation phenomena typical of SMMs have been observed in this family of oxamato-bridged trinuclear and hexanuclear species.

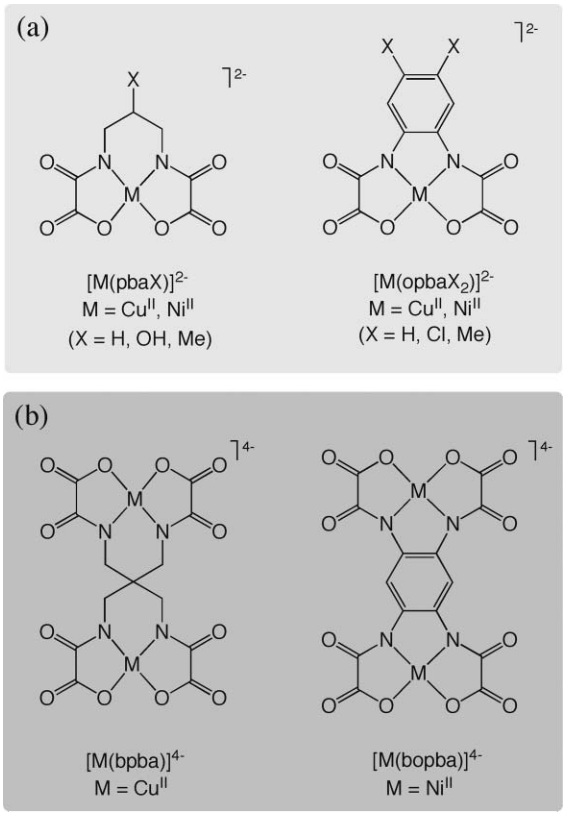

Scheme 1 Self-assembling metal oxamato complexes resulting from the coordination of aliphatic and aromatic group-substituted bis- and tetrakis(oxamato) ligands to late 3d divalent metal ions: (a) mono- and (b) dinuclear complexes (M = Cu and Ni).

As far as the oxamato-bridged coordination polymers are concerned, some of the first examples of molecule-based magnets were obtained by following the rational design strategy developed by Kahn.[26,27] In this pioneering work, mononuclear oxamato copper(II) complexes were used as bis(bidentate) ligands toward fully solvated metal ions for the preparation of both hetero-bimetallic one-[26] and two-dimensional[27] compounds which order ferromagnetically through interchain and interplanar interactions, respectively (Fig. 2 and 3).

Such an approach was proved to be successful for the first time by the Kahn's group for the series of oxamato-bridged $M^{II}Cu^{II}$ chains (M = Mn, Fe, Co and Ni) prepared from the mononuclear copper(II) complex $[Cu^{II}(pbaOH)]^{2-}$ [H_4pbaOH = *N*,*N*′-2-hydroxy-1,3-propylenebis(oxamic acid)] [Fig. 2(a)]. In fact, some members of this series show a long-range 3D ferromagnetic order of the ferrimagnetic chains (T_C = 4.6–9.5 K)[26a,c,d,h] while others order antiferromagnetically (T_N = 2.4–3.4 K),[26d,g] depending on the nature of the interchain hydrogen bonds involving crystallization water molecules. These results show how subtle differences in the crystal packing of the chains dramatically influence the 3D magnetic behavior and, at the same time, they underline the limits of the 1D strategy to obtain molecule-based magnets because of the difficulty to control the interchain interactions. On the contrary, the series of oxamato-bridged $M^{II}Cu^{II}$ chains (M = Mn and Co) prepared from the mononuclear copper(II) complex $[Cu^{II}(opba)]^{2-}$ [H_4opba = *N*,*N*′-1,2-phenylenebis(oxamic acid)] [Fig. 2(b)] behave in general as almost ideal 1D ferrimagnets with no long-range magnetic ordering above 2.0 K, showing that the chains are well isolated in the crystal lattice.[26l,27a] However, no slow magnetic relaxation phenomena typical of SCMs have been observed in this family of oxamato-bridged heterobimetallic chains.

In a subsequent work, Kahn and Stumpf prepared the corresponding oxamato-bridged $M^{II}{}_2Cu^{II}{}_3$ planes (M = Mn, Fe, Co and Ni) with either a parallel [Fig. 3(a)] or a perpendicular interlocked

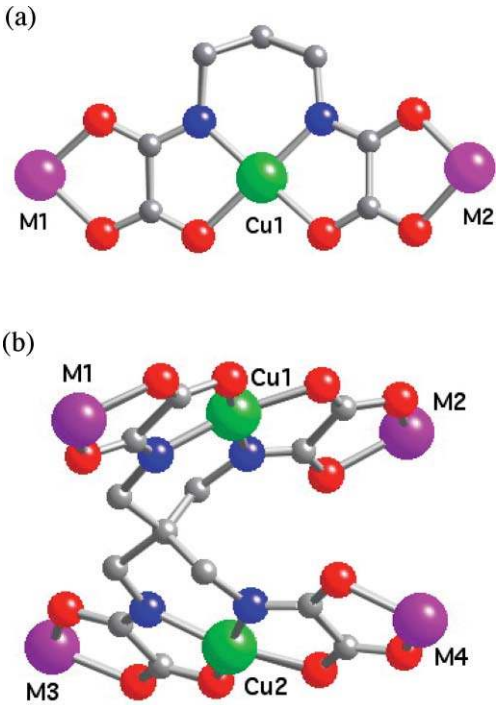

Fig. 1 Structures of the 0D coordination compounds prepared by using the copper(II) complexes $[Cu(pba)]^{2-}$ and $[Cu_2(bpba)]^{4-}$ as precursors: (a) trinuclear $Cu^{II}M^{II}{}_2$ and (b) hexanuclear $Cu^{II}{}_2M^{II}{}_4$ complexes (M = Cu, Ni, Co and Mn). Color coding: gray = carbon, blue = nitrogen, red = oxygen.

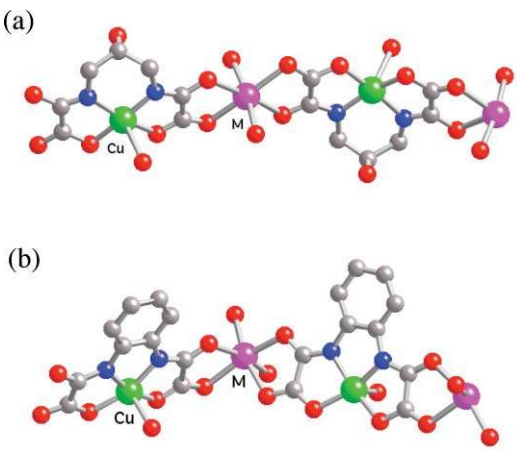

Fig. 2 Structures of the 1D coordination polymers prepared by using the copper(II) complexes $[Cu(pbaOH)]^{2-}$ and $[Cu(opba)]^{2-}$ as precursors: (a) linear and (b) zigzag $M^{II}Cu^{II}$ chains (M = Mn, Fe, Co and Ni). See Fig. 1 for color coding.

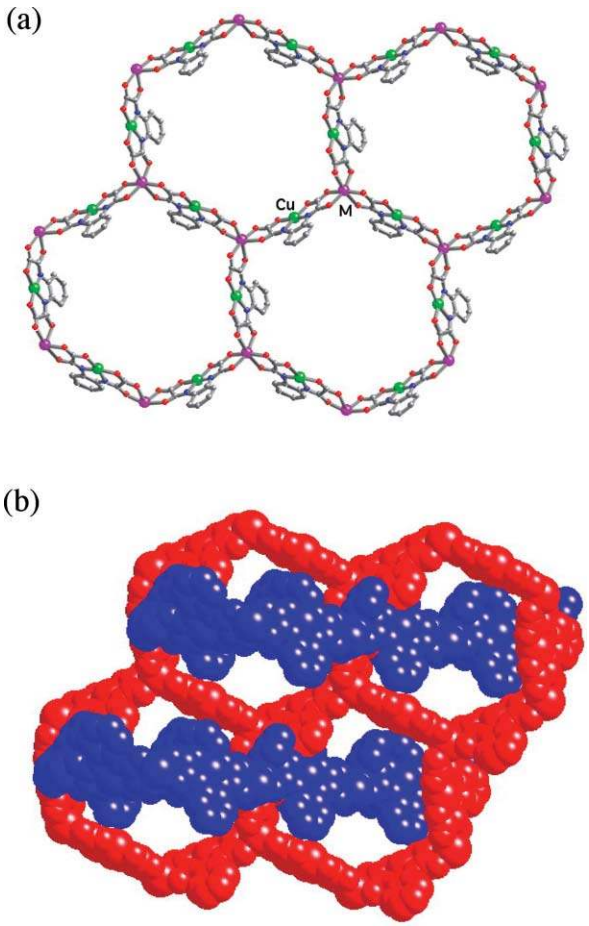

Fig. 3 Structures of the 2D coordination polymers prepared by using the copper(II) complex $[Cu(opba)]^{2-}$ as precursor: (a) parallel and (b) interpenetrated honeycomb hexagonal $M^{II}_2Cu^{II}_3$ planes (M = Mn, Fe, Co and Ni). See Fig. 1 for color coding.

disposition of the honeycomb hexagonal planes [Fig. 3(b)] depending on the nature of the countercation, either alkaline[27n] and tetraalkylammonium cations[27a,j–m] or *N*-alkyl-substituted pyridinium derivatives of nitronyl nitroxide radicals,[27b–i,o] respectively. These ferrimagnetic planes indeed possess higher ordering temperatures than their 1D analogues (T_C up to 37 K), showing the need to increase the dimensionality in order to obtain high-T_C molecule-based magnets. In general, the $Mn^{II}_2Cu^{II}_3$ planes are soft magnets (H_c = 10 Oe),[27a–c] whereas the $Co^{II}_2Cu^{II}_3$ ones are very hard magnets (H_c = 25 kOe).[27d] The observed differences in coercivity are likely related to the strong magnetic anisotropy of the Co^{II} ion in a distorted octahedral environment because of the orbital contribution of the $^4T_1$ ground state, when compared to the magnetically isotropic Mn^{II} ion with no first-order orbital contribution in the ^6A ground state. In terms of future applications of these molecular magnetic materials, the coercivity (property which confers a memory effect to the material) is as important as the critical temperature.

Inspired by this work, we and others have extended this well-known "complex-as-ligand" (CAL) approach by using oligonuclear complexes of late first-row transition metal ions, from mono- to trinuclear, with related aromatic-substituted mono-, di- and tris(oxamato) ligands as building blocks.[28–37] In the following, the metallosupramolecular design strategy will be described first and then, a brief account of our main findings concerning the structure and magnetism of the oligonuclear precursors and the resultant metallosupramolecular complexes of variable nuclearity and dimensionality will be given. As a matter of fact, this strategy has provided the first examples of oxamato-bridged SMMs and SCMs, and it has also allowed the entry to higher dimensionality oxamato-bridged molecule-based magnets. Finally, the potential of our approach in the design and synthesis of addressable, multifunctional molecular materials for future applications in molecular electronics and nanotechnology will be outlined.

The *leitmotiv* that has guided our work is rightly expressed in the voice of the Portuguese most famous poet, Fernando Pessoa:

"*Deve haver, no mais pequeno poema de um poeta, qualquer coisa por onde se note que existiu Homero. (…) A novidade, em si mesma, nada significa, se não houver nela uma relação com o que a precedeu. Nem, propriamente, há novidade sem que haja essa relaçáo. Saibamos distinguir o novo do estranho; o que, conhecendo o conhecido, o transforma e varia, e o que aparece de fora sem conhecimiento de coisa nenhuma*"

(extracted from *Paginas Íntimas e Auto Interpretação* and *Estranheza e Novidade*; in *Ricardo Reis-Prosas*).†

This Perspective is meant to be an affectionate tribute to the late Olivier Kahn, our particular Homer in the Odyssey of supramolecular magnetism.

Metallosupramolecular design strategy

Molecular-programmed self-assembly of ligands

In the search for ligand design for the construction of self-assembling metallosupramolecular oxamato complexes with first-row transition metal ions, we have focused on the acid derivatives of the ligands *N*-phenyloxamato (H_2pma), *N*,*N*′-1,3-phenylenebis(oxamato) (H_4mpba), *N*,*N*′-1,4-phenylenebis-(oxamato) (H_4ppba) and *N*,*N*′,*N*″-1,3,5-benzenetriyltris-(oxamato) (H_6mpta), together with their methyl-substituted analogues (Scheme 2). This series of suitable designed aromatic polyoxamato ligands (APOXAs) consists of a somewhat rigid polymethyl-substituted benzene scaffold with multiple oxamato binding sites of various substitution pattern (polytopic ligands). The great versatility of these ligands lies on the variety of binding modes of each class. Depending on the number of oxamato metal binding sites, from one to three, they can be classified as ligands of the first- (L = pma, pmaMe, $pmaMe_2$ and $pmaMe_3$), second- (L = mpba, mpbaMe, $mpbaMe_3$ and ppba), and third-generation (L = mpta), respectively.

According to the basic principles of metallosupramolecular chemistry, the nuclearity and topology of the complexes resulting from the interaction between this new family of APOXA ligands

† "In the smallest poem of a poet, something must advertise us of Homer's existence. Novelty has no significance if it does not rely on experiences from the past. There is properly no novelty if there is no such a relationship. We shall distinguish the new from the strange; the one being aware of what is already known, make it changed and vary it, from the one that comes from outside without knowledge".

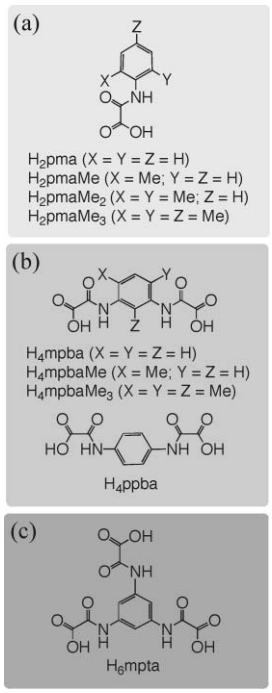

Scheme 2 Aromatic-substituted polyoxamato ligands of various preferred coordination modes: (a) mono-, (b) di- and (c) trinucleating.

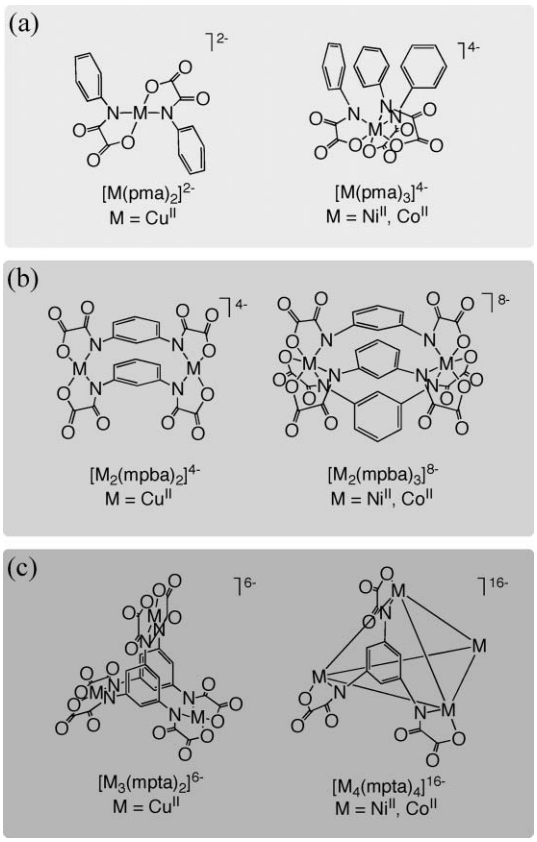

Scheme 3 Self-assembling metallosupramolecular oxamato complexes with late 3d divalent metal ions of different preferred coordination geometries: (a) double and triple, *trans* and *cis* mononuclear complexes, (b) double- and triple-stranded dinuclear metallacyclic complexes and (c) tri- and tetranuclear metallacyclic cages (M = Cu, Ni and Co).

and first-row transition metal ions would depend mainly on the topicity of the ligand and on the preferred coordination geometry of the metal ion. Thus, they can act as mono-, di- and trinucleating ligands when coordinating to late 3d divalent metal ions, from Cu^{II} to Co^{II}, through the amide-nitrogen and carboxylate-oxygen atoms of the oxamate groups affording the corresponding oligonuclear oxamato complexes, from mono- to tetranuclear, depending on the four-coordinate square-planar or six-coordinate octahedral metal coordination geometry (Scheme 3). This situation clearly contrasts with that of the related opba and bopba ligands which commonly act in mono- and dinucleating chelating ways respectively, toward late (Cu and Ni) 3d divalent metal ions (Scheme 1).[24a,c,e] In that case, the achievement of mono- and dinuclear metal complexes is due entirely to the structure of the extensively preorganized ligand and consequently, the self-assembly process is structurally trivial.[2] In a certain manner, the work which is the subject of the present review constitutes the transition from classic (Werner-type) to supramolecular coordination chemistry (metallosupramolecular chemistry) by using oxamato ligands.

Molecular-programmed self-assembly of metalloligands

A variety of complex metallosupramolecular assemblies with predictable structures can be rationally designed and synthesized from these self-assembled oligonuclear oxamato complexes with late 3d divalent metal ions (M = Cu, Ni and Co). In fact, they can act as ligands (metalloligands) because of their potential metal binding ability toward other middle and late 3d divalent metal ions (M' = Cu, Ni, Co and Mn) through the two outer *cis* carbonyl-oxygen atoms of the oxamato groups, as shown earlier for the related copper(II)–opba mononuclear complex. In this sense, APOXA ligands offer a kind of double programming according to the terminology of metallosupramolecular chemistry. The first level of ligand programming allows the coordination to the M^{II} ions (M = Cu, Ni and Co) through the bidentate *N*,*O*-oxamato donor set to give mono- or oligonuclear metallacyclic complexes, either metallacyclophanes, metallacryptands, or metal cages. The second level of ligand programming resides precisely on the free carbonyl oxygen atoms which allow these self-assembled metallosupramolecular species to be used as ligands (metalloligands) toward other M'^{II} ions (M' = Cu, Ni, Co and Mn). Such outer coordination has been rarely exploited for metallacryptands (helicates and *meso*-helicates), whereby the inner coordination to give metallacryptates is commonly observed.[38] This metal binding ability may play a relevant role in the alternative organization of helicates and *meso*-helicates and, moreover, it may be advantageously used for the elaboration of higher order metallosupramolecular assemblies.

This molecular-programmed approach based on ligand design allows the rational preparation of coordination polymers of variable dimensionality as well as polynuclear compounds of variable nuclearity when using blocking ligands in the coordination sphere of the coordinated metal ion to preclude polymerization. In each case, the resulting polynuclear complexes, from tri- to

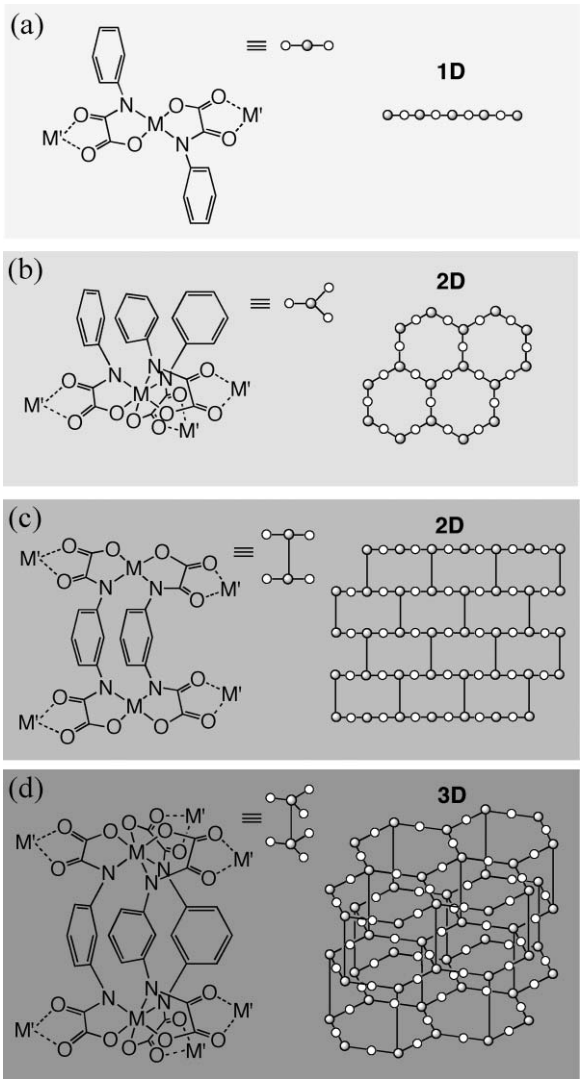

Scheme 4 Oxamato-bridged bimetallic coordination polymers resulting from the metal-mediated self-assembly of the metallosupramolecular anionic complexes with middle and late 3d divalent metal ions: (a) 1D ribbonlike chains, (b) 2D honeycomb and (c) brick-wall planes, and (d) 3D honeycomb frameworks (M = Cu, Ni and Co; M′ = Cu, Ni, Co and Mn).

octanuclear, constitute the basic structural units for the construction of the corresponding *n*D (*n* = 1–3) coordination polymers, whose topology would depend on the coordination mode of the metalloligand (Scheme 4). The use of di- and trinuclear oxamato complexes as metalloligands has received limited attention compared to the more common mononuclear ones; however, it constitutes a step further toward the preparation of high-nuclearity and high-dimensionality coordination compounds, as recently demonstrated for the aforementioned dicopper(II)–bpba complex [Scheme 1(c)].[24b]

Metalloligands

Mononuclear complexes

Two bidentate L ligands (L = pmaMe, pmaMe$_2$ and pmaMe$_3$) coordinate to one Cu^{II} ion in a stoichiometric ratio *SR* = 1/2 to yield the anionic mononuclear copper(II) complexes [Cu^{II}L$_2$]$^{2-}$ of global complexity *GC* = 1 + 2 = 3.[28b] The crystal structures of the tetraphenylphosphonium and sodium salts (Ph$_4$P)$_2$[Cu(pmaMe$_2$)$_2$]·4H$_2$O and Na$_2$[Cu(pmaMe$_3$)$_2$]·6H$_2$O, show the occurrence of four-coordinate square-planar copper(II) dianions with a *trans* arrangement of the two polymethyl-substituted phenyloxamato ligands [Fig. 4(a) and 5(a)].[28b,29b] The phenyl rings in both compounds are practically perpendicular

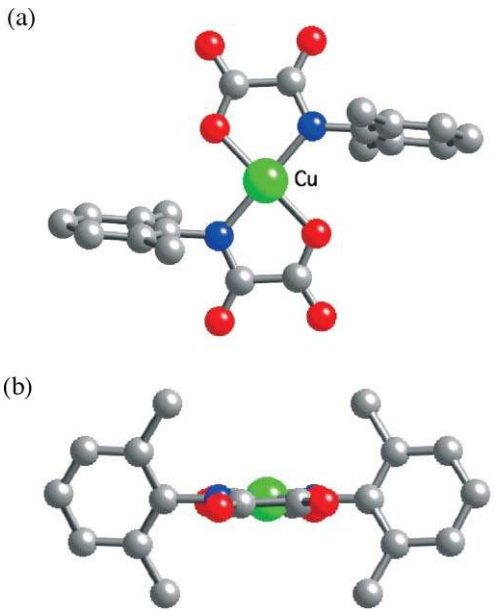

Fig. 4 (a) Top and (b) side views of the anionic mononuclear unit of (Ph$_4$P)$_2$[Cu(pmaMe$_2$)$_2$]·4H$_2$O with the atom labelling of the metal atom (hydrogen atoms are omitted for clarity) [symmetry code: (I) = $-x$, $1-y$, $1/2-z$]. See Fig. 1 for color coding.

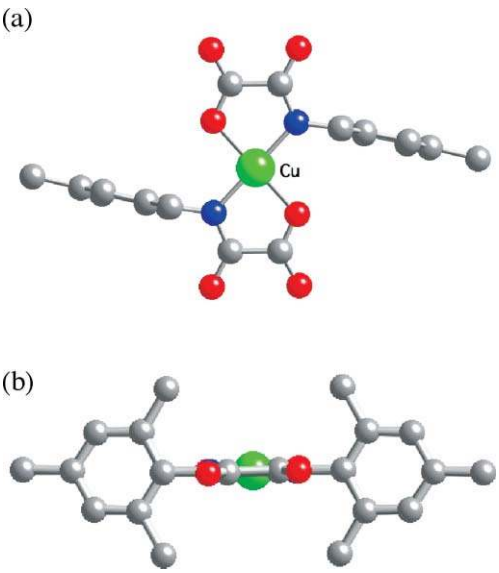

Fig. 5 (a) Top and (b) side views of the anionic mononuclear unit of Na$_2$[Cu(pmaMe$_3$)$_2$]·6H$_2$O with the atom labelling of the metal atom (hydrogen atoms are omitted for clarity) [symmetry code: (I) = $-x$, $1-y$, $1/2-z$]. See Fig. 1 for color coding.

to the oxamate groups [dihedral angles of 82.7(6) and 82.1(4)°] in order to avoid the steric repulsions between the 2- and 6-methyl substituents and the carbonyl-oxygen atoms [Fig. 4(b) and 5(b)]. More likely, the alternative *cis* arrangement of the oxamato ligands is precluded because of the steric effects between the methyl substituents from the two facing phenyl groups. The shortest intermolecular copper-copper separation through the hydrogen-bonded crystallization water molecules in $(Ph_4P)_2[Cu(pmaMe_2)_2]\cdot 4H_2O$ is 14.276(5) Å, whereas that through the coordinated sodium ions in $Na_2[Cu(pmaMe_3)_2]\cdot 6H_2O$ is 7.267(8) Å.

Complexes $(Ph_4P)_2[Cu(pmaMe_2)_2]\cdot 4H_2O$ and $Na_2[Cu(pmaMe_3)_2]\cdot 6H_2O$ exhibit a Curie-Weiss magnetic behavior characteristic of four-coordinate square-planar Cu^{II} d^9 ($S_{Cu} = 1/2$) ions with very weak Weiss constants [$\theta = zJ'S_{Cu}(S_{Cu} + 1)/3k_B$ within the molecular field approximation].[28b] The almost zero value of the intermolecular magnetic coupling in $(Ph_4P)_2[Cu(pmaMe_2)_2]\cdot 4H_2O$ ($-zJ' < 0.01$ cm^{-1}) is consistent with magnetically-isolated Cu^{II} ions which are well separated from each other due to the presence of the bulky Ph_4P^+ organic cations. Instead, the low but non-negligible value of the intermolecular magnetic coupling in $Na_2[Cu(pmaMe_3)_2]\cdot 6H_2O$ ($-zJ' = 0.25$ cm^{-1}) is associated to weak dipolar and/or antiferromagnetic exchange interactions between the Cu^{II} ions through the coordinated Na^I cations.

Double-stranded dinuclear complexes

The tetradentate ligation to a single metal center being precluded with the two bis(bidentate) L ligands (L = mpba, $mpbaMe_3$ and ppba), they self-assemble side-by-side with two Cu^{II} ions in a stoichiometric ratio $SR = 2/2$ to yield the anionic double-stranded dinuclear copper(II) complexes $[Cu^{II}_2L_2]^{4-}$ of global complexity $GC = 2 + 2 = 4$.[28] The two square-planar copper(II)-bis(oxamato) moieties are connected by a double phenylene skeleton of either *meta*- or *para*-substitution patterns to give a metallacyclic core structure of meta- or paracyclophane type respectively, as illustrated by the crystal structures of the sodium salts $Na_4[Cu_2(mpba)_2]\cdot 10H_2O$ and $Na_4[Cu_2(ppba)_2]\cdot 11H_2O$ [Fig. 6(a) and 7(a)].[30a,b] The values of the intradimer copper-copper distance through the two *m*- and *p*-phenylenediamidate bridges are 6.822(2) and 7.910(1) Å for $Na_4[Cu_2(mpba)_2]\cdot 10H_2O$ and $Na_4[Cu_2(ppba)_2]\cdot 11H_2O$, respectively.

In both cases, the π–π interactions between the two parallel phenylene rings [Fig. 6(b) and 7(b)] are likely to play a role during the metal-directed self-assembly process leading to the formation of the double-stranded, square-planar dicopper(II) metallacyclophane complexes. The average values of the C–C distance between the two facing phenylene rings which are connected by the two N–Cu–N linkages are 3.38 and 3.46 Å for $Na_4[Cu_2(mpba)_2]\cdot 10H_2O$ and $Na_4[Cu_2(ppba)_2]\cdot 11H_2O$ respectively, values which are slightly shorter than that of the van der Waals contact (3.5 Å). Hence, the $Cu_2(m\text{-}N_2C_6H_4)_2$ metacyclophane moiety in $Na_4[Cu_2(mpba)_2]\cdot 10H_2O$ has an approximate C_{2v} symmetry, with the mean basal planes of the copper atoms being almost perpendicular to those of the *m*-phenylene rings [dihedral angles in the range 72.1(3)–82.0(3)°] [Fig. 6(c)]. However, the copper basal planes are far from being perpendicular to the *para*-substituted phenylene planes for $Na_4[Cu_2(ppba)_2]\cdot 11H_2O$ [dihedral angles of 57.4(2) and 62.9(2)°]. The deviations from

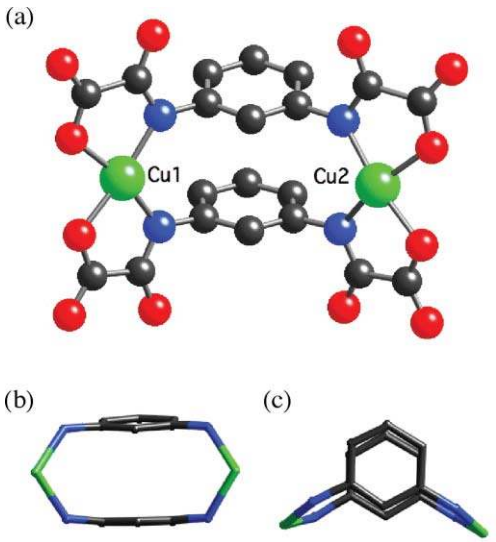

Fig. 6 (a) Perspective view of the anionic dinuclear unit of $Na_4[Cu_2(mpba)_2]\cdot 10H_2O$ with the atom labelling of the metal atoms (hydrogen atoms are omitted for clarity). (b) Front and (c) top views of the metacyclophane-type metallacyclic core. See Fig. 1 for color coding.

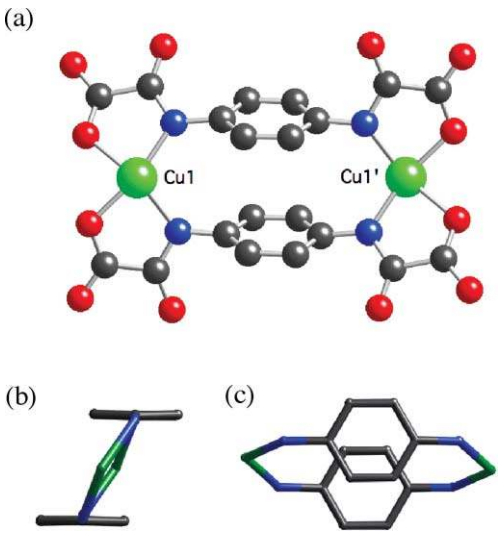

Fig. 7 (a) Perspective view of the anionic dinuclear unit of $Na_4[Cu_2(ppba)_2]\cdot 11H_2O$ with the atom labelling of the metal atoms (hydrogen atoms are omitted for clarity) [symmetry code: (I) = $-x$, $-y$, $-z$]. (b) Side and (c) top views of the paracyclophane-type metallacyclic core. See Fig. 1 for color coding.

an ideal D_{2h} symmetry for the $Cu_2(p\text{-}N_2C_6H_4)_2$ paracyclophane moiety may be caused by the favorable π–π interactions in the parallel-displaced configuration of the *p*-phenylene groups [Fig. 7(c)].

In spite of the relatively large intramolecular copper–copper separations, moderate ferro- ($J = +17$ cm^{-1}) to strong antiferromagnetic ($J = -81$ cm^{-1}) couplings are observed between the two Cu^{II} ions ($S_{Cu} = 1/2$) for $Na_4[Cu_2(mpba)_2]\cdot 10H_2O$ and $Na_4[Cu_2(ppba)_2]\cdot 11H_2O$ respectively, leading thus to $S = 0$ and $S = 1$ ground states [$H = -JS_1\cdot S_2$ with $S_1 = S_2 = S_{Cu}$].[30a,b] The ferro- or antiferromagnetic nature of the exchange interaction results from

a spin polarization mechanism through the extended π-conjugated bond system of the phenylene spacers with *meta*- and *para*-substitution patterns respectively, as confirmed by density functional theory (DFT) calculations on the triplet and broken symmetry (BS) singlet ground spin states of $Na_4[Cu_2(mpba)_2]\cdot 10H_2O$ and $Na_4[Cu_2(ppba)_2]\cdot 11H_2O$, respectively (Fig. 8).[30a,b] These two dicopper(II) metallacyclophanes constitute unique examples of spin control in transition metal complexes through the topology of the bridging ligand.[39]

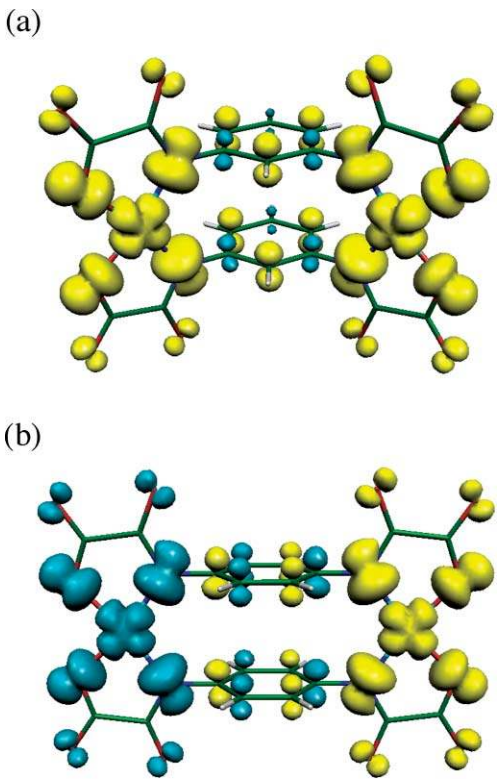

Fig. 8 Perspective views of the calculated spin density distribution for the (a) triplet and (b) BS singlet ground spin states in $Na_4[Cu_2(mpba)_2]\cdot 10H_2O$ and $Na_4[Cu_2(ppba)_2]\cdot 11H_2O$, respectively. Yellow and blue contours represent positive and negative spin densities, respectively. The isodensity surface corresponds to a value of 0.0015 $e\ a_0^{-3}$.

Triple-stranded dinuclear complexes

When using Ni^{II} or Co^{II} instead of Cu^{II} ions, the side-by-side self-assembly of three bis(bidentate) L ligands (L = mpba and mpbaMe) and two metal ions ($SR = 2/3$) yields the related anionic triple-stranded dinuclear nickel(II) and cobalt(II) complexes $[M_2L_3]^{8-}$ of larger global complexity ($GC = 2 + 3 = 5$).[28b] The two trigonally-distorted octahedral metal(II)-tris(oxamato) moieties of opposite chirality (ΔΛ form) are connected by three *m*-phenylene spacers to give a metallamacrobicyclic core of the cryptand type, as illustrated by the crystal structures of the sodium salts $Na_4[M_2(mpba)_3]\cdot 12H_2O$ (M = Ni and Co) [Fig. 9(a)].[28b,31] The intradimer meta-metal distances through the three *m*-phenylenediamidate bridges are 6.829(4) (M = Ni) and 6.866(5) Å (M = Co).

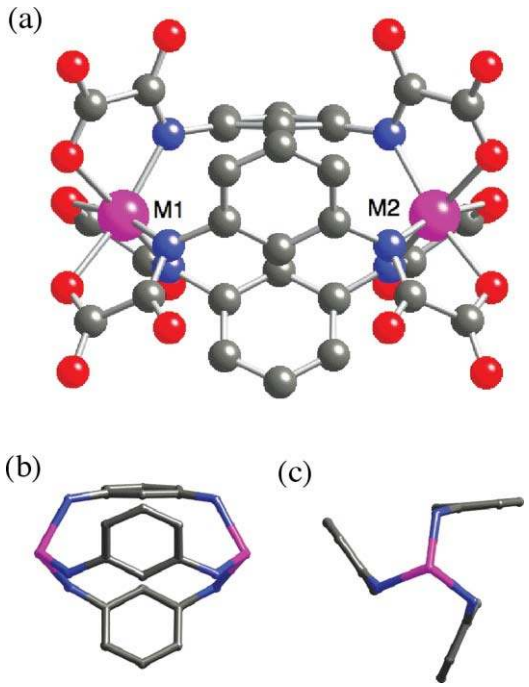

Fig. 9 (a) Perspective view of the anionic dinuclear unit of $Na_8[M_2(mpba)_3]\cdot 12H_2O$ (M = Ni and Co) with the atom labelling of the metal atoms (hydrogen atoms are omitted for clarity) [symmetry code: (I) = $-y + 1, x - y, z$; (II) = $-x + y + 1, -x + 1, z$]. (b) Front and (c) side views of the meso-helicate-type metallacryptand core. See Fig. 1 for color coding.

In each case, the unique formation of triple-stranded, octahedral dinickel(II) and dicobalt(II) metallacryptand complexes of *meso*-helicate type, so-called mesocates, is favored because of the relatively short and rigid character of the phenylene spacer which prevents helical twisting of the nonplanar bridging ligands around the metal centers.[38] Indeed, the helical wrapping of the three ligands around the two metal centers would alternately lead to dinuclear helicates with D_{3d} molecular symmetry, instead of the actual dinuclear mesocates with C_{3h} molecular symmetry. Unlike what occurs in the dicopper(II) metallacyclophane analogue, the aromatic groups in the dinickel(II) and dicobalt(II) metallacryptand complexes $Na_4[M_2(mpba)_3]\cdot 12H_2O$ (M = Ni and Co) are not stacked in a parallel manner but arranged in an edge-to-face fashion with a weak C–H···π interaction [Fig. 9(b) and (c)]. Within the $M_2(m\text{-}N_2C_6H_4)_3$ (M = Ni and Co) metallacryptand core, the values of the torsion angle (α) around the M–N–C–C bonds are 93.6(7) (M = Ni) and 94.0(5)° (M = Co). They are within the range of those reported for the $Cu_2(m\text{-}N_2C_6H_4)_2$ metallacyclophane core in $Na_4[Cu_2(mpba)_2]\cdot 10H_2O$ [α = 73.6(7)–97.9(7)°].

Complexes $Na_4[M_2(mpba)_3]\cdot 12H_2O$ (M = Ni and Co) exhibit $S = 2$ (M = Ni) and $S = 3$ (M = Co) ground states as a result of the moderate to weak ferromagnetic coupling [J = +3.6 (M = Ni) and +1.3 cm^{-1} (M = Co)] between the two high-spin Ni^{II} d^8 ($S_{Ni} = 1$) or Co^{II} d^7 ($S_{Co} = 3/2$ and $L_{Co} = 1$) ions having either a significant axial zero-field-splitting ($D = -3.5$ cm^{-1}) [$H = -JS_1\cdot S_2 + D(S_{z1}^2 + S_{z2}^2)$ with $S_1 = S_2 = S_{Ni}$] or an important spin–orbit coupling ($\lambda = -145$ cm^{-1}) [$H = -JS_1\cdot S_2 + \alpha\lambda(L_1\cdot S_1 + L_2\cdot S_2) + \Delta(L_{z1}^2 - L_{z2}^2)$ with $S_1 = S_2 = S_{Co}$ and

$L_1 = L_2 = L_{Co}$], respectively.[28b,31] In both cases, the observed ferromagnetic interaction results from the sign alternation of the spin density in the *meta*-substituted phenylene spacers, as confirmed by density functional theory (DFT) calculations on the quintet and septet ground spin states of $Na_4[Ni_2(mpba)_3]\cdot 12H_2O$ and $Na_4[Co_2(mpba)_3]\cdot 12H_2O$, respectively (Fig. 10). The ferromagnetic behavior in these dinickel(II) and dicobalt(II) metallacryptands is rather exceptional for transition metal complexes.[39] At this respect, the successful extension of the spin polarization approach to ferromagnetism which was checked first in the related dicopper(II) metallacyclophane supports the general validity of this strategy for late 3d metal ions.

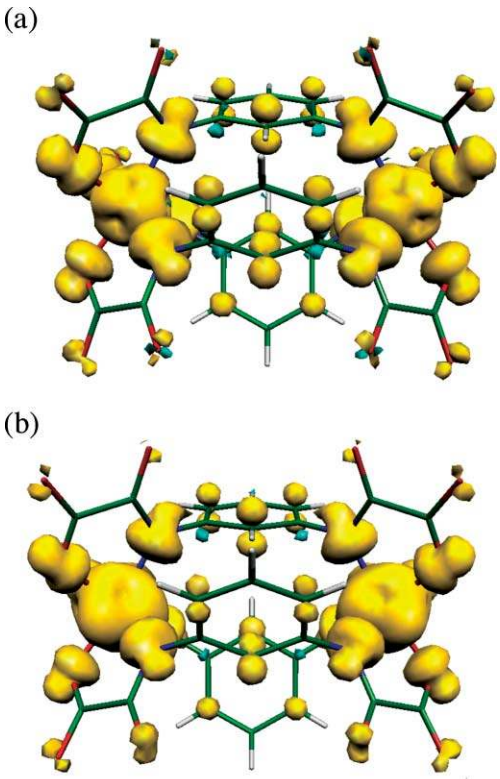

Fig. 10 Perspective views of the calculated spin density distribution for the (a) quintet and (b) heptet ground spin states in $Na_8[Ni_2(mpba)_3]\cdot 12H_2O$ and $Na_8[Co_2(mpba)_3]\cdot 12H_2O$, respectively. Yellow and blue contours represent positive and negative spin densities, respectively. The isodensity surface corresponds to a value of 0.0015 $e\ a_0^{-3}$.

Trinuclear complexes

Two tris(bidentate) L ligands (L = mpta) self-assemble side-by-side with three Cu^{II} ions ($SR = 3/2$) to yield the anionic trinuclear copper(II) complex $[Cu^{II}{}_3L_2]^{6-}$ of global complexity $GC = 3 + 2 = 5$.[28a] The three square-planar copper(II)-bis(oxamato) moieties are connected by a double 1,3,5-benzenetriyl skeleton, as illustrated by the crystal structure of the potassium salt $K_6[Cu_3(mpta)_2]\cdot 11H_2O$ [Fig. 11(a)].[28a,37b] This leads to a unique triangular metallacyclophane cage with a roughly C_{3h} molecular symmetry. Hence, within the $Cu_3(1,3,5\text{-}N_3C_6H_3)_2$ metallacyclophane core, there is an almost perfect face-to-face alignment of the two benzene rings from each C_3-symmetric bridging ligand around the three-fold molecular

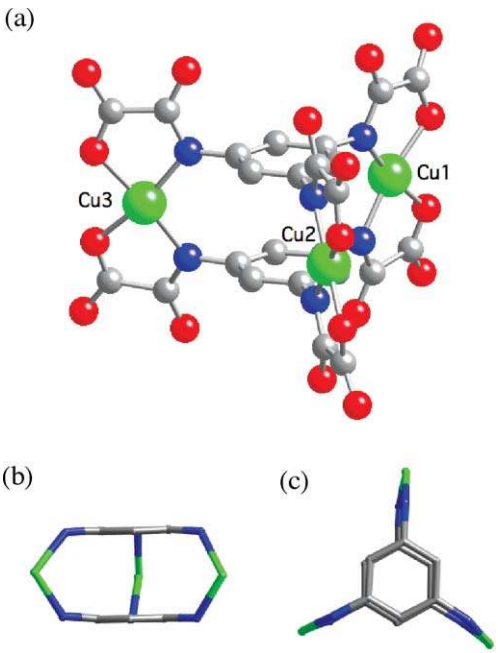

Fig. 11 (a) Perspective view of the anionic trinuclear unit of $K_6[Cu_2(mpta)_2]\cdot 11H_2O$ with the atom labelling of the metal atoms (hydrogen atoms are omitted for clarity). (b) Front and (c) top views of the 1,3,5-cyclophane-type metallacyclic core. See Fig. 1 for color coding.

axis, with the mean basal planes of the copper atoms being almost perpendicular to those of the benzene rings [Fig. 11(b) and (c)]. The values of the dihedral angle vary in the range 82.5(3)–87.6(3)°. They are closer to 90° than in the dicopper(II) metallacyclophane analogue $Na_4[Cu_2(mpba)_2]\cdot 10H_2O$ [dihedral angles in the range 72.1(3)–82.0(3)°]. The average value of the C–C distance between the two facing benzenetriyl rings which are connected by the three N–Cu–N linkages is 3.25 Å, a value which is smaller than that in $Na_4[Cu_2(mpba)_2]\cdot 10H_2O$ (3.38 Å). The values of the intratrimer copper–copper distances through the two 1,3,5-benzenetriyltriamidate bridges are in the range 6.911(2)–7.057(1) Å.

Complex $K_6[Cu_3(mpta)_2]\cdot 11H_2O$ exhibits a $S = 3/2$ ground spin state which results from the moderate ferromagnetic coupling ($J = +11.8\ cm^{-1}$) between the three Cu^{II} ions ($S_{Cu} = 1/2$) across the two 1,3,5-benzenetriyl spacers [$H = -J(S_1\cdot S_2 + S_1\cdot S_3 + S_2\cdot S_3)$ with $S_1 = S_2 = S_3 = S_{Cu}$].[28a,37b] The ferromagnetic interaction in this tricopper(II) metallacyclic triangle is certainly due to spin polarization effects through the aromatic spacers of *meta*-substitution pattern, as for the related dicopper(II) metacyclophane ($J = +16.8\ cm^{-1}$). We are currently searching for tetranickel(II) and tetracobalt(II) metallacyclic tetrahedra with the benzenetriyl-tris(oxamate) ligand (L = mpta) [Scheme 3(c)], which would possess larger spin and magnetic anisotropy values, as potential candidates to SMMs. This approach to ferromagnetism based on the interaction between spin densities of different signs issued from spin polarization effects is particularly appealing. It has, however, received limited attention in the context of the polynuclear metal complexes,[39] in contrast to its extensive use by organic chemists working with high-spin organic molecules (polyradicals) or mixed organic–inorganic molecules (metal–polyradical complexes).[40,41]

High-nuclearity coordination compounds

Penta- and hexanuclear complexes

The dicopper(II) complexes $[Cu^{II}_2L_2]^{4-}$ (L = mpba, mpbaMe$_3$ and ppba) can act as tetrakis(bidentate) or tris(bidentate) ligands toward either four or three coordinatively unsaturated copper(II) or nickel(II) complexes, $[Cu^{II}L']^{2+}$ (L′ = Me$_4$en and Me$_5$dien) and $[Ni^{II}L']^{2+}$ (L′ = Me$_3$tacden and cyclam) respectively,‡ to give the cationic homo- and heterometallic, hexa- and pentanuclear compounds of general formula $[(Cu^{II}_2L_2)(Cu^{II}L')_4]^{4+}$ and $[(Cu^{II}_2L_2)(Ni^{II}L')_3]^{2+}$, respectively (Scheme 5 and 6).[28]

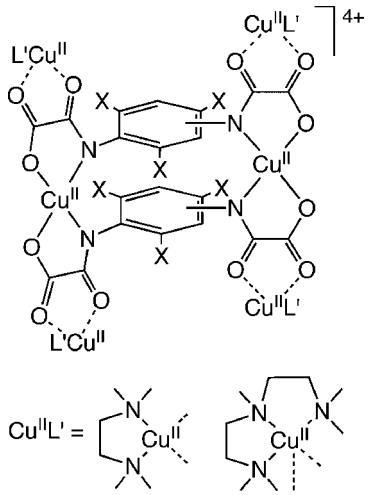

Scheme 5 Structural formula of the homometallic hexanuclear $M^{II}_2M'^{II}_4$ complexes (M = M′ = Cu).

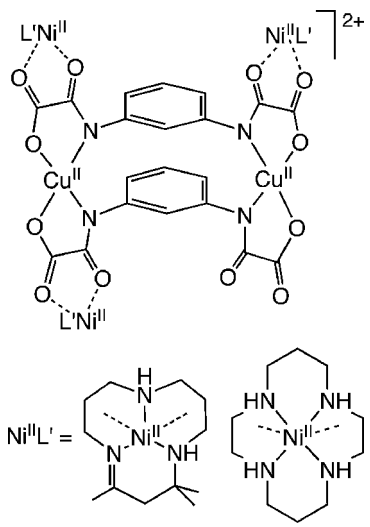

Scheme 6 Structural formula of the heterometallic pentanuclear $M^{II}_2M'^{II}_3$ complexes (M = Cu and M′ = Ni).

The hexacopper(II) cations have a "dimer-of-trimers" structure with an overall [2 × 2] ladder-type architecture, as illustrated by the crystal structures of $\{[Cu_2(mpbaMe_3)_2(H_2O)_2][Cu(Me_5dien)]_4\}(ClO_4)_4\cdot12H_2O$ and $\{[Cu_2(ppba)_2][Cu(Me_5dien)]_4\}(ClO_4)_4$ [Fig. 12(a) and 13(a)].[33] Each Cu^{II}_6 entity is made up of two oxamato-bridged Cu^{II}_3 linear units acting as 'rails' which are connected through either two *meta*- or two *para*-substituted phenylenediamidate bridges serving as 'rungs' between the central copper atoms, leading thus to Cu^{II}_2 metallacyclic cores of the *meta*- and *para*-cyclophane type, respectively [Fig. 12(c) and 13(c)]. Within the Cu^{II}_2 metacyclophane core of $\{[Cu_2(mpbaMe_3)_2(H_2O)_2][Cu(Me_5dien)]_4\}(ClO_4)_4\cdot12H_2O$, there exists a slight twisting of the two benzene rings from the perfect face-to-face alignment due to the steric hindrance between the equivalent methyl groups of each ring [Fig. 12(c)]. In contrast, the two benzene rings are not eclipsed but slightly glided perpendicularly to the copper–copper vector within the Cu^{II}_2 paracyclophane core of $\{[Cu_2(ppba)_2][Cu(Me_5\text{-}dien)]_4\}(ClO_4)_4$ [Fig. 13(c)]. The values of the intramolecular distance between the two central copper atoms through the double *m*- and *p*-phenylenediamidate bridges for $\{[Cu_2(mpbaMe_3)_2(H_2O)_2][Cu(Me_5dien)]_4\}(ClO_4)_4\cdot12H_2O$ and $\{[Cu_2(ppba)_2][Cu(Me_5dien)]_4\}(ClO_4)_4$ are 7.087(19) and 8.059(2) Å respectively, while the average values of the intramolecular distance between the central and peripheral copper atoms through the oxamato bridge are 5.330(15) and 5.340(5) Å, respectively.

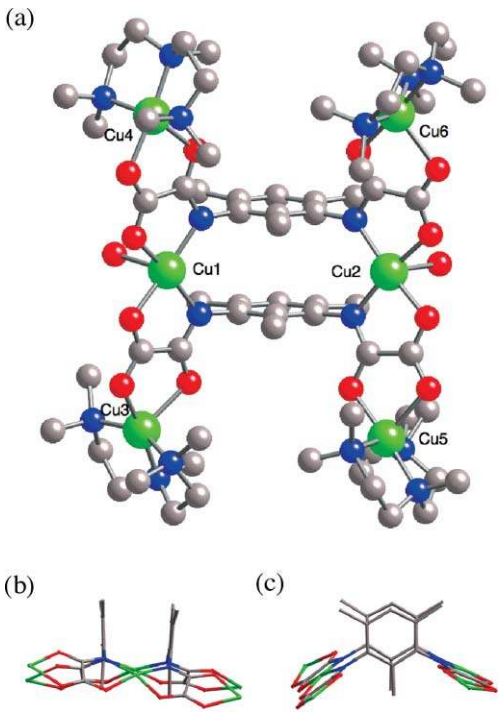

Fig. 12 (a) Perspective view of the cationic hexanuclear unit of $\{[Cu_2(mpbaMe_3)_2(H_2O)_2][Cu(Me_5dien)]_4\}(ClO_4)_4\cdot12H_2O$ with the atom labelling of the metal atoms (hydrogen atoms are omitted for clarity). (b) Side and (c) top views of the hexanuclear skeleton standing out the dinuclear metallacyclophane core. See Fig. 1 for color coding.

The pentanuclear copper(II)-nickel(II) cations exhibit instead a "dimer-plus-trimer" structure with an incomplete [2 × 2] ladder-type architecture, as illustrated by the crystal structure of $[Ni(cyclam)]\{[Cu_2(mpba)_2][Ni(cyclam)]_3\}(ClO_4)_4\cdot6H_2O$, whereby

‡ *Ligand abbreviations:* Me$_4$en = *N*,*N*,*N*′,*N*′-tetramethylethylenediamine, Me$_5$dien = *N*,*N*,*N*′,*N*′,*N*″-pentamethyldiethylenetriamine, dipn = dipropylenetriamine, Me$_3$tacden = 2,4,4-trimethyl-1,5,9-triazacyclododec-1-ene and cyclam = 1,4,8,11-tetraazacyclotetradecane.

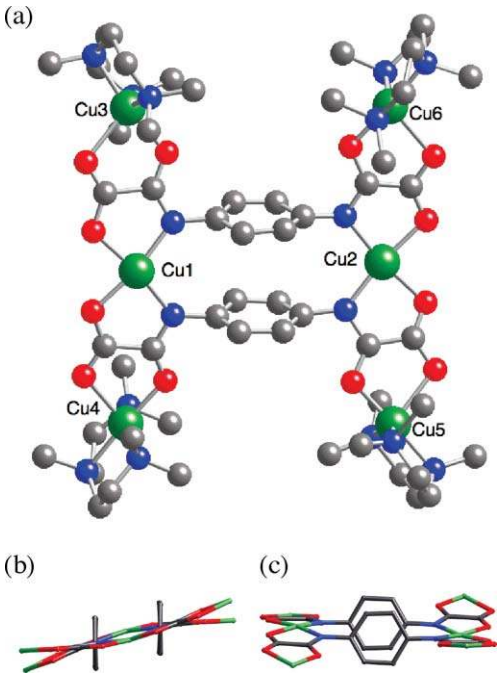

Fig. 13 (a) Perspective view of the cationic hexanuclear unit of $\{[Cu_2(ppba)_2][Cu(Me_5dien)]_4\}(ClO_4)_4$ with the atom labelling of the metal atoms (hydrogen atoms are omitted for clarity). (b) Side and (c) top views of the hexanuclear skeleton standing out the dinuclear metallacyclophane core. See Fig. 1 for color coding.

mononuclear square-planar nickel(II) complexes are present as additional counter-cations [Fig. 14(a)].[33b] Each $Cu^{II}_2Ni^{II}_3$ entity is made up of oxamato-bridged $Cu^{II}Ni^{II}$ and $Cu^{II}Ni^{II}_2$ linear units connected through two *meta*-phenylenediamidate bridges between the two copper atoms to afford a Cu^{II}_2 metacyclophane core [Fig. 14(c)]. Within the Cu^{II}_2 metacyclophane core, there is a rather large distortion from the parallel face-to-face alignment of the two benzene rings [dihedral angle of 15.2(4)°] [Fig. 14(b)], as compared to the situation observed in the hexanuclear copper(II) analogue $\{[Cu_2(mpbaMe_3)_2(H_2O)_2][Cu(Me_5dien)]_4\}(ClO_4)_4\cdot 12H_2O$. This reflects the non-equivalence of the two central copper atoms in the pentanuclear compound as a consequence of the absence of a peripheral nickel coordination site. The value of the intramolecular distance between the two copper atoms through the double *m*-phenylenediamidate bridge is 6.937(7) Å, while those between the copper and the nickel atoms through the oxamato bridge average 5.319(4) Å.

The magnetic properties of this family of oxamato-bridged, homo- and heterometallic $M^{II}_2M'^{II}_x$ complexes [M = Cu; M′ = Cu (x = 4) and Ni (x = 3)] with dinuclear metallacyclophane cores are consistent with their distinct "dimer-of-trimers" and "dimer-plus-trimer" structures, respectively [$H = -J(S_{1A}\cdot S_{3A} + S_{1A}\cdot S_{4A} + S_{2B}\cdot S_{5B} + S_{2B}\cdot S_{6B}) - J'S_{1A}\cdot S_{2B}$ with $S_{1A} = S_{2B} = S_M$ and $S_{3A} = S_{4A} = S_{5B} = S_{6B} = S_{M'}$] [Scheme 7(a) and 8(a)].[33] The moderate to strong antiferromagnetic intratrimer and/or intradimer coupling between the Cu^{II} and M'^{II} ions through the oxamato bridge [$-J$ = 81.3–288.3 (M′ = Cu) and 111.6–158.0 cm^{-1} (M′ = Ni)] agrees with that found in related oxamato-bridged trinuclear copper(II) ($-J$ = 89–356.6 cm^{-1})[25l,m,r] and di- and trinuclear copper(II)-nickel(II) complexes ($-J$ = 104.2–108.0 cm^{-1}).[25n,q] Within the dinuclear metacyclophane core, a moderate ferromagnetic coupling operates between the two Cu^{II} ions through the double *m*-phenylenediamidate bridge (J' = 1.7–15.5 cm^{-1}), while a strong antiferromagnetic coupling is

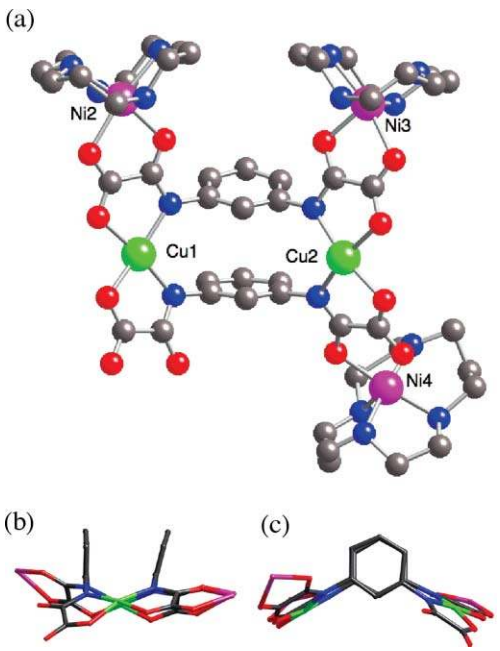

Fig. 14 (a) Perspective view of the cationic pentanuclear unit of $[Ni(cyclam)]\{[Cu_2(mpba)_2][Ni(cyclam)]_3\}(ClO_4)_4\cdot 6H_2O$ with the atom labelling of the metal atoms (hydrogen atoms are omitted for clarity). (b) Side and (c) top views of the pentanuclear skeleton standing out the dinuclear metallacyclophane core. See Fig. 1 for color coding.

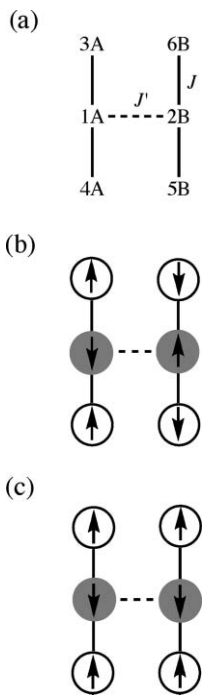

Scheme 7 (a) Spin coupling pattern and (b) and (c) spin topologies for the hexanuclear $M^{II}_2M'^{II}_4$ complexes (M = M′ = Cu) with $J < 0$ and either $J' < 0$ or $J' > 0$, respectively.

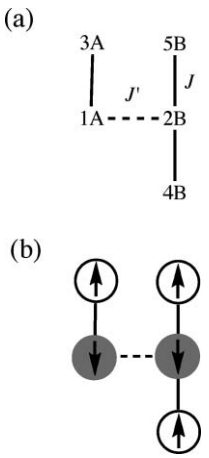

Scheme 8 (a) Spin coupling pattern and (b) spin topology for the pentanuclear $M^{II}_2M'^{II}_3$ complexes (M = Cu and M′ = Ni) with $J < 0$ and $J' > 0$.

mediated by the double *p*-phenylenediamidate bridge within the paracyclophane core ($J' = -120.6$ cm^{-1}). The moderate to strong, either ferro- or antiferromagnetic couplings, depending on the *meta* (L = mpba and mpbaMe$_3$) or *para* (L = ppba) substitution pattern of the bridging ligand respectively, agrees both in sign and magnitude with those found in the related dicopper(II) complexes $Na_4[Cu_2(mpba)_2]\cdot 8H_2O$ ($J' = +16.8$ cm^{-1}), $Na_4[Cu_2(mpbaMe_3)_2]\cdot 9H_2O$ ($J' = +11.0$ cm^{-1}) and $Na_4[Cu_2(ppba)_2]\cdot 11H_2O$ ($J' = -81.0$ cm^{-1}). Overall, this situation indicates that the spin polarization mechanism also applies for the propagation of the exchange interaction in both the hexanuclear copper(II) and pentanuclear copper(II)–nickel(II) complexes.[33b]

The spin of the ground state in these two series of hexa- and pentanuclear $M^{II}_2M'^{II}_x$ complexes [M = Cu; M′ = Cu ($x = 4$) and Ni ($x = 3$)] with dinuclear meta- (L = mpba and mpbaMe$_3$) and paracyclophane (L = ppba) cores can be rationally interpreted based on the concept of ferro- (FC) and antiferromagnetic (AC) coupling units. Hence, the Cu^{II}_2 paracyclophane entity acts as a "robust" AC unit between the two Cu^{II}_3 fragments ($S_A = S_B = 2S_{Cu} - S_{Cu} = 1/2$), leading to a low-lying singlet spin state for the Cu^{II}_6 complexes ($S = S_A - S_B = 0$) [Scheme 7(b)]. On the contrary, the Cu^{II}_2 metacyclophane entities act as more or less "robust" FC units between the two Cu^{II}_3 fragments ($S_A = S_B = 1/2$), leading to a triplet ground spin state for the Cu^{II}_6 ($S = S_A + S_B = 1$) complexes [Scheme 7(c)]. Similarly, quintet ground spin states are obtained for the corresponding $Cu^{II}_2Ni^{II}_3$ ($S = S_A + S_B = 2$) complexes, whereby the Cu^{II}_2 (L = mpba) metacyclophane core acts as a "robust" FC unit between the $Cu^{II}Ni^{II}$ ($S_A = S_{Ni} - S_{Cu} = 1/2$) and $Cu^{II}Ni^{II}_2$ ($S_B = 2S_{Ni} - S_{Cu} = 3/2$) fragments [Scheme 8(b)]. This represents a successful extension of the concept of magnetic coupling units to inorganic complexes which has been used earlier to control the spin in polyradicals and metal–polyradical complexes.[40,41]

Complex $\{[Cu_2(mpba)_2][Ni(Me_3tacden)]_3\}(ClO_4)_2\cdot 10H_2O$ has a strongly anisotropic $S = 2$ ground state, reflecting both the single-ion magnetic anisotropy of the high-spin Ni^{II} ions in a distorted trigonal-bipyramidal coordination geometry (local anisotropy) and the low symmetry of the "dimer-plus-trimer" structure (structural anisotropy) which precludes the cancellation of the resulting total magnetic anisotropy. Interestingly, this pentanuclear copper(II)-nickel(II) complex exhibits slow magnetic relaxation effects at low temperatures ($T_B < 5.0$ K) which are reminiscent of SMMs.[28b] However, the calculated values of the relaxation time (τ) for $\{[Cu_2(mpba)_2][Ni(Me_3tacden)]_3\}(ClO_4)_2\cdot 10H_2O$ deviate appreciably from the Arrhenius law characteristic of a thermally-activated mechanism, $\tau = \tau_0 \exp(E_a/k_BT)$, which should give a straight line in the semilog plot of τ *vs.* $1/T$ (Fig. 15). The calculated values of the activation energy ($E_a = 79.9$ cm^{-1}) and the pre-exponential factor ($\tau_0 = 5.5 \times 10^{-15}$ s) are physically meaningless, as expected for a classical spin glass system.[42] Thus, the E_a value is very high and the τ_0 value is abnormally low when compared to the values previously reported for other SMMs.[20] Alternatively, the analysis of the temperature dependence of the relaxation time on the basis of the Vogel–Fulcher law for weakly interacting molecules, $\tau = \tau_0 \exp[E_a/k_B(T - T_0)]$, gave now physically meaningful values of both the preexponential factor ($\tau_0 = 6.8 \times 10^{-7}$ s) and the activation energy ($E_a = 6.8$ cm^{-1}) with a non-negligible intermolecular interaction parameter ($T_0 = 3.0$ K) (solid line in Fig. 15).[42a] Overall, this suggests a picture of weak ferromagnetically coupled $S = 2$ $Cu^{II}_2Ni^{II}_3$ SMMs which would be responsible for the unique magnetic relaxation dynamics observed in $\{[Cu_2(mpba)_2][Ni(Me_3tacden)]_3\}(ClO_4)_2\cdot 10H_2O$ ("cluster glass" behavior).[42b]

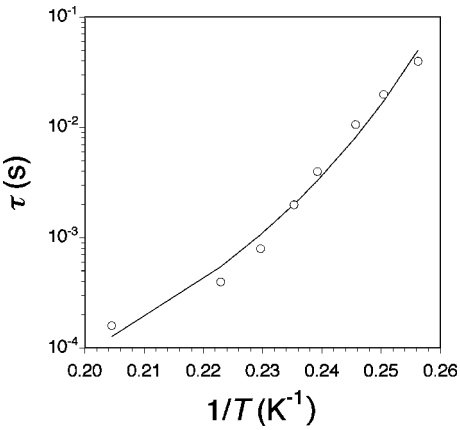

Fig. 15 Arrhenius plot for $\{[Cu_2(mpba)_2][Ni(Me_3tacden)]_3\}(ClO_4)_2\cdot 10H_2O$ (the solid line is the best-fit curve).

Octanuclear complexes

When acting as hexakis(bidentate) ligands, the dicopper(II), dinickel(II) and dicobalt(II) complexes $[M^{II}_2L_3]^{8-}$ (M = Cu, Ni and Co; L = mpba and mpbaMe) coordinate to six coordinatively unsaturated copper(II) or nickel(II) complexes, $[Cu^{II}L']^{2+}$ (L′ = Me$_5$dien) and $[Ni^{II}L']^{2+}$ (L′ = dipn) respectively,‡ to give the cationic homo- and heterometallic octanuclear compounds of general formula $[(M^{II}_2L_3)(Cu^{II}L')_6]^{4+}$ and $[(Ni^{II}_2L_3)(Ni^{II}L')_6]^{4+}$ (Scheme 9).[28b]

The octanuclear metal(II)–copper(II) cations have a "dimer-of-tetramers" structure with an overall double-propeller architecture, as illustrated by the crystal structures of $Na_2\{[M_2(mpba)_3][Cu(Me_5dien)]_6\}(ClO_4)_6\cdot xH_2O$ [M = Cu ($x = 12$), Ni ($x = 17$) and Co ($x = 22$)], whereby two sodium

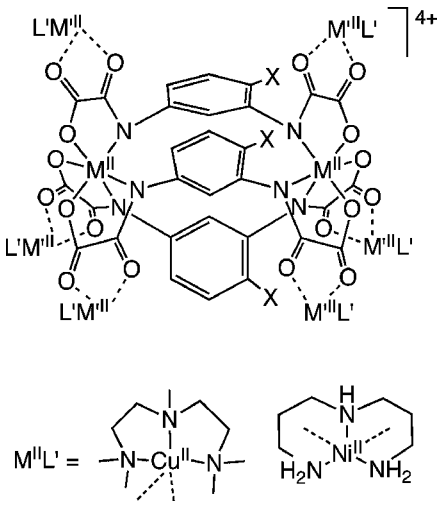

Scheme 9 Structural formula of the homo- and heterometallic octanuclear $M^{II}_2M'^{II}_6$ complexes (M = Cu, Ni and Co; M′ = Cu and Ni).

ions are present as additional counter-cations [Fig. 16(a)].[34a,d] Each $M^{II}_2Cu^{II}_6$ entity (M = Cu, Ni and Co) with C_{3h} molecular symmetry is made up of two oxamato-bridged, heterochiral propeller-like $M^{II}Cu^{II}_3$ units (Δ and Λ enantiomers) which are connected through three *meta*-phenylenediamidate bridges between the central metal atoms to give a dinuclear metallamacrobicyclic core of the cryptand-type [Fig. 16(b) and (c)]. Because of the presence of a mirror plane perpendicular to the molecular three-fold axis, this achiral M^{II}_2 (M = Cu, Ni and Co) metallacryptand core is of *meso*-helicate-type, like those of the related dinickel(II) and dicobalt(II) complexes $Na_8[M_2(mpba)_3]\cdot 12H_2O$ (M = Ni and Co) with a strictly zero helical twist angle of the two metal sites of opposite Δ and Λ chiralities around the M–M vector. Interestingly, the M–N distances [2.050(6) (M = Cu), 2.062(5) (M = Ni) and 2.096(7) Å (M = Co)] are similar to the M–O ones [2.121(5) (M = Cu), 2.102(5) (M = Ni) and 2.116(8) Å (M = Co)]. This indicates a rather unique dynamic Jahn–Teller effect for the coordination environment of the two central copper atoms in $Na_2\{[Cu_2(mpba)_3][Cu(Me_5dien)]_6\}(ClO_4)_6\cdot 12H_2O$, whereby the elongation spreads randomly over the three axes, in contrast to the more common elongated or compressed Jahn–Teller distorted octahedral Cu^{II} ions, with four short and two long metal–ligand bond lengths or *vice versa*. The values of the intramolecular M–M distance between the two central metal atoms through the triple *m*-phenylenediamidate bridge are 6.592(3) (M = Cu), 6.846(5) (M = Ni) and 6.768(4) Å (M = Co), while those of the intramolecular M–Cu distance between the central and peripheral metal atoms through the oxamato bridge are 5.418(7) (M = Cu), 5.435(5) (M = Ni) and 5.441(6) Å (M = Co).

The octanuclear nickel(II) cations also have a "dimer-of-tetramers" structure with an overall double-propeller architecture, as illustrated by the crystal structure of $\{[Ni_2(mpba)_3][Ni(dipn)(H_2O)]_6\}(ClO_4)_4\cdot 12.5H_2O$ [Fig. 17(a)].[34b] Each Ni^{II}_8 entity is made up of two oxamato-bridged, heterochiral propeller-like Ni^{II}_4 units (Δ and Λ enantiomers) [Fig. 17(b)], which are connected through three *meta*-substituted phenylenediamidate bridges between the central metal atoms to give a Ni^{II}_2 metallacryptand core of the

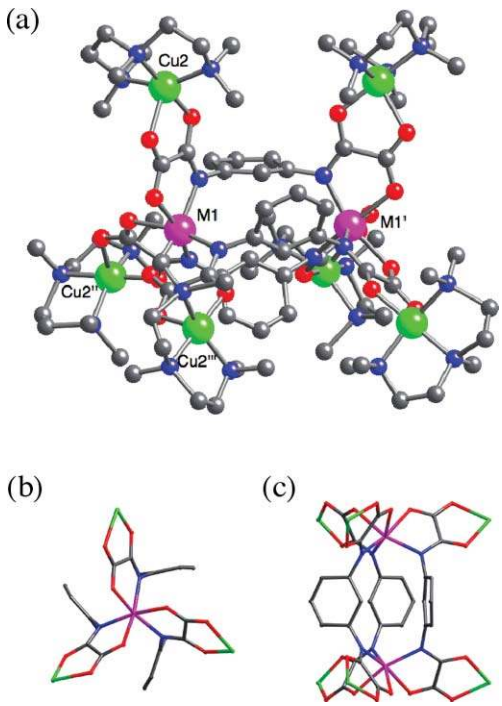

Fig. 16 (a) Perspective view of the cationic octanuclear unit of $Na_2\{[M_2(mpba)_3][Cu(Me_5dien)]_6\}(ClO_4)_6\cdot nH_2O$ [M = Cu (*n* = 12), Ni (*n* = 17) and Co (*n* = 22)] with the atom labelling of the metal atoms (hydrogen atoms are omitted for clarity) [symmetry codes: (I) = 1 − *x* − *y*, 1 − *x*, 1/2 − *z*; (II) = −*y* + 1, *x* − *y*, *z*; (III) = −*x* + *y* + 1, −*x* + 1, *z*]. (b) Side and (c) top views of the octanuclear skeleton standing out the dinuclear metallacryptand core. See Fig. 1 for color coding.

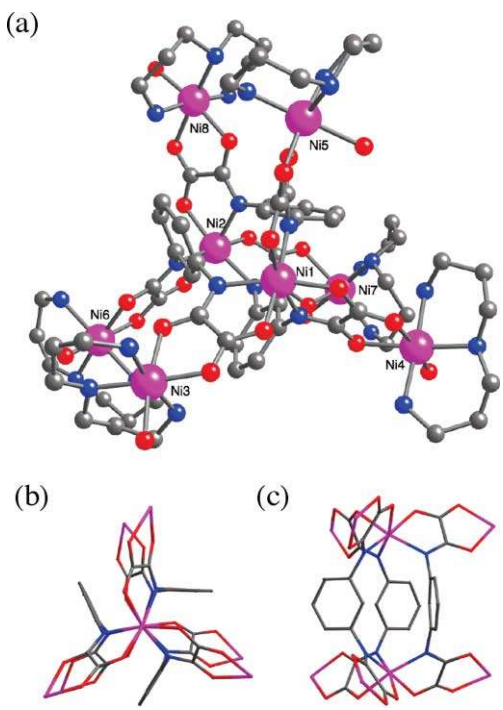

Fig. 17 (a) Perspective view of the octanuclear unit of $\{[Ni_2(mpba)_3][Ni(dipn)(H_2O)]_6\}(ClO_4)_4\cdot 12.5H_2O$ with the atom labelling of the metal atoms (hydrogen atoms are omitted for clarity). (b) Side and (c) top views of the octanuclear skeleton standing out the dinuclear metallacryptand core. See Fig. 1 for color coding.

meso-helicate-type [Fig. 17(c)]. In contrast to what happens in $Na_2\{[Ni_2(mpba)_3][Cu(Me_5dien)]_6\}(ClO_4)_6\cdot 17H_2O$, the two central metal sites of opposite Δ and Λ chiralities are slightly tilted from each other by 4.7(5)° around the Ni1–Ni2 vector and consequently, the dinuclear metallacryptand core has a pseudo C_{3h} molecular symmetry. As a whole, the octanuclear unit has a reduced C_1 molecular symmetry because of the presence among the six peripheral metal atoms of both *mer* (Ni3, Ni4, Ni6 and Ni8) and *fac* (Ni5 and Ni7) isomers with respect to the conformation of the dipn ligand, whereas all six peripheral copper atoms are *mer* isomers in the heterooctanuclear nickel(II)-copper(II) analogue. The value of the intramolecular Ni–Ni distance between the two central metal atoms through the triple *m*-phenylenediamidate bridge is 6.829(4) Å, while those of the intramolecular Ni–Ni distances between the central and peripheral metal atoms through the oxamato bridge are in the range 5.446(2)–5.487(6) Å.

The magnetic properties of this family of oxamato-bridged, homo- and heterometallic $M^{II}_2M'^{II}_6$ complexes (M = Cu, Ni and Co; M′ = Cu and Ni) with dinuclear metallacryptand cores are consistent with its "dimer-of-tetramers" structure [$H = -J(S_{1A}\cdot S_{3A} + S_{1A}\cdot S_{4A} + S_{1A}\cdot S_{5A} + S_{2B}\cdot S_{6B} + S_{2B}\cdot S_{7B} + S_{2B}\cdot S_{8B}) - J'S_{1A}\cdot S_{2B}$ with $S_{1A} = S_{2B} = S_M$ and $S_{3A} = S_{4A} = S_{5A} = S_{6B} = S_{7B} = S_{8B} = S_{M'}$] [Scheme 10(a)].[34] Thus, complexes $Na_2\{[M_2(mpba)_3][Cu(Me_5dien)]_6\}(ClO_4)_6\cdot xH_2O$ [M = Cu (x = 12), Ni (x = 17) and Co (x = 22)] show a moderate to weak antiferromagnetic coupling [J' = −28.0 (M = Cu), −0.20 (M = Ni) and −1.0 cm^{-1} (M = Co)] between the two moderately strong antiferromagnetically-coupled $M^{II}Cu^{II}_3$ star-shaped units [J = −57.0 (M = Cu), −39.1 (M = Ni) and −17.0 cm^{-1} (M = Co)]. Instead, complexes $\{[Ni_2L_3][Ni(dipn)(H_2O)]_6\}(ClO_4)_4\cdot 12.5H_2O$ (L = mpba and mpbaMe) exhibit a weak ferromagnetic coupling [J' = +3.1 (L = mpba) and +2.1 cm^{-1} (L = mpbaMe)] between the two moderately strong antiferromagnetically-coupled Ni^{II}_4 star-shaped units [J = −26.6 (L = mpba) and −26.3 cm^{-1} (L = mpbaMe)]. The attenuation of the antiferromagnetic intratetramer coupling between the M^{II} and M'^{II} ions through the oxamato bridges when replacing Cu^{II} ($S_{Cu} = 1/2$) by high-spin Ni^{II} ($S_{Ni} = 1$) and Co^{II} ($S_{Co} = 3/2$) as central and/or peripheral metal ions along this series is as expected because of the increase in the number of unpaired electrons on the metal center. Yet, the moderate to weak, either antiferro- or ferromagnetic intertetramer coupling operating between the M^{II} ions (M = Cu, Ni and Co) within the M^{II}_2 metallacryptand core contrasts with that reported for the related dinickel(II) and dicobalt(II) metallacryptand complexes [J' = +3.6 (M = Ni) and +1.3 cm^{-1} (M = Co)]. Overall, this situation indicates that the spin delocalization effects dominate over the spin polarization ones, favoring an antiferromagnetic interaction in the octanuclear metal(II)–copper(II) complexes.

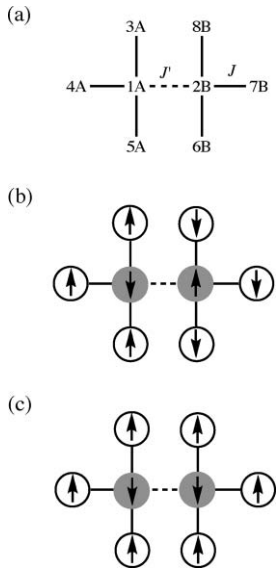

Scheme 10 (a) Spin coupling pattern and (b) and (c) spin topologies for the octanuclear $M^{II}_2M'^{II}_6$ complexes (M = Cu, Ni and Co; M′=Cu and Ni) with $J < 0$ and either $J' < 0$ or $J' > 0$, respectively.

Hence, these two series of $M^{II}_2M'^{II}_6$ complexes (M = Cu, Ni and Co; M′ = Cu and Ni) with dinuclear metallacryptand cores have different ground spin states depending on the combination of the M and M′ ions [Scheme 10(b) and (c)]. In the series of $M^{II}_2Cu^{II}_6$ (M = Cu, Ni and Co) complexes, the M^{II}_2 metallacryptand cores act as more or less "robust" AC units between the two $M^{II}Cu^{II}_3$ star fragments [$S_A = S_B = 3S_{Cu} - S_M = 1$ (M = Cu), $\frac{1}{2}$ (M = Ni) and 0 (M = Co)], leading to a singlet ground state for the whole $M^{II}_2Cu^{II}_6$ molecule ($S = S_A - S_B = 0$) [Scheme 10(b)]. In contrast, a nonet ground state is achieved for the Ni^{II}_8 ($S = S_A + S_B = 4$) complexes, whereby the Ni^{II}_2 metallacryptand core acts as a more or less "robust" FC unit between the Ni^{II}_4 star fragments ($S_A = S_B = 3S_{Ni} - S_{Ni} = 2$) [Scheme 10(c)]. Complex $\{[Ni_2(mpba)_3][Ni(dipn)(H_2O)]_6\}(ClO_4)_4\cdot 12.5H_2O$ behaves thus as a ferromagnetically coupled dimer of $S = 2$ Ni^{II}_4 units with a high-spin ground state ($S = 4$).[34b] The moderate axial magnetic anisotropy ($D = -0.23$ cm^{-1}) ultimately reflects both the single-ion magnetic anisotropy of the high-spin Ni^{II} ions in a distorted octahedral coordination geometry (local anisotropy) and the low symmetry of the "dimer-of-tetramers" structure (structural anisotropy). Similarly to the pentanuclear copper(II)–nickel(II) complex $\{[Cu_2(mpba)_2][Ni(Me_3tacden)]_3\}(ClO_4)_2\cdot 10H_2O$, this octanuclear nickel(II) complex also exhibits slow magnetic relaxation effects at low temperatures ($T_B < 3.6$ K) which are reminiscent of a "cluster glass" dynamics.[34b]

The analysis of the temperature dependence of the relaxation time for $\{[Ni_2(mpba)_3][Ni(dipn)(H_2O)]_6\}(ClO_4)_4\cdot 12.5H_2O$ on the basis of the Vogel–Fulcher law gave values of 3.0×10^{-7} s and 5.9 cm^{-1} for τ_0 and E_a respectively, with a T_0 value of 2.4 K (Fig. 18).[28b] The calculated E_a value compares reasonably well with

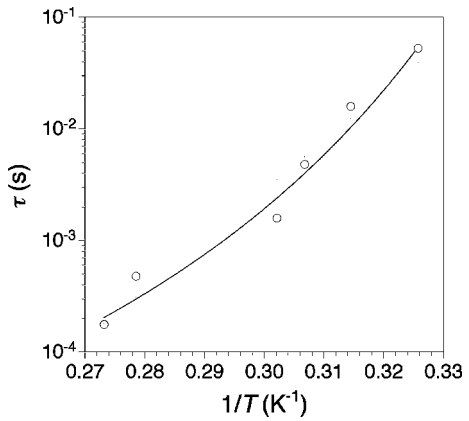

Fig. 18 Arrhenius plot for $\{[Ni_2(mpba)_3][Ni(dipn)(H_2O)]_6\}(ClO_4)_4\cdot 12.5H_2O$ (the solid line is the best-fit curve).

that estimated assuming that the slow relaxation stems exclusively from the $S = 4$ ground spin state. Thus, the activation energy for the magnetization reversal between the two lowest $M_S = \pm 4$ energy levels may be related to the axial anisotropy parameter ($D = -0.23$ cm^{-1}) of the $S = 4$ ground state of the Ni^{II}_8 molecule by $E_a = -DS^2$, giving an estimated value of E_a of 3.7 cm^{-1}. On the other hand, the calculated value of T_0 suggests a picture of weak antiferromagnetically coupled $S = 4$ Ni^{II}_8 SMMs which would be responsible for the unique magnetic relaxation dynamics. This is consistent with the crystal structure which shows that the Ni^{II}_8 molecules weakly interact with each other through a variety of hydrogen bonding interactions involving both the coordinated and crystallization water molecules. We guess that the existence of some kind of hydrogen-bond disorder, most likely due to the partial loss of crystallization water molecules, would be ultimately responsible for the observed spin glass behavior.[42]

Complexes $\{[Cu_2(mpba)_2][Ni(Me_3tacden)]_3\}(ClO_4)_2 \cdot 10H_2O$ and $\{[Ni_2(mpba)_3][Ni(dipn)(H_2O)]_6\}(ClO_4)_4 \cdot 12.5H_2O$ thus constitute the first examples of oxamato-bridged SMMs exhibiting slow magnetic relaxation behavior at low temperatures; their relaxation dynamics present a glassy behavior typical of cluster glasses because of the presence of weak intermolecular interactions. At this respect, it deserves to be noted that silica-based mesoporous materials have recently been employed as support hosts for $\{[Ni_2(mpba)_3][Ni(dipn)(H_2O)]_6\}(ClO_4)_4 \cdot 12.5H_2O$.[34c] The incorporation and aggregation of the Ni^{II}_8 molecules into the ordered mesoporous silica led to oligomeric $[Ni^{II}_8]_n$ aggregates of greater values of the spin ($S = 4n$) and blocking temperatures (T_B = 4.5–10.5 K) than those of the crystalline material. In this case, the existence of a wide distribution of aggregates with different conformation and association degrees (size distribution) and the presence of weak interactions between the aggregates led also to an exotic spin glass magnetic behavior for this family of host–guest hybrid nanocomposite materials which is reminiscent of that of multidispersed superparamagnetic nanoparticles.

Nonanuclear complexes

When acting as a hexakis(bidentate) ligand, the tricopper(II) complex $[Cu^{II}_3L_2]^{6-}$ (L = mpta) coordinates to six coordinatively unsaturated copper(II) complexes $[Cu^{II}L']^{2+}$ (L′ = Me_4en and Me_5dien)‡ to give the cationic homometallic nonanuclear compounds of general formula $[(Cu^{II}_3L_2)(Cu^{II}L')_6]^{6+}$ (Scheme 11).[28a] The nonanuclear copper(II) cations have a "trimer-of-trimers" structure with an overall cylinder-like architecture, as illustrated by the crystal structures of $\{[Cu_3(mpta)_2(H_2O)_2][Cu(Me_4en)]_6\}(ClO_4)_6$ and $\{[Cu_3(mpta)_2(H_2O)_2][Cu(Me_5dien)]_6\}(ClO_4)_6 \cdot 9H_2O$ [Fig. 19(a) and (b)].[28a,37] Each Cu^{II}_9 entity is made up of three oxamato-bridged, linear Cu^{II}_3 units, which are connected through two 1,3,5-substituted benzenetriylamidate bridges between the central copper atoms to give a trinuclear metallacyclic core of the 1,3,5-cyclophane-type [Fig. 19(b) and 20(b)]. Within the Cu^{II}_3 metallacyclophane core, the two coplanar benzene rings are not eclipsed but somewhat twisted resulting in a greater overall torsion than that found in the tricopper(II) metacyclophane complex $K_6[Cu_3(mpta)_3] \cdot 11H_2O$. The values of the Cu–N–C–C torsion angles (α) vary in the range 44.6(5)–66.2(5)° for $\{[Cu_3(mpta)_2(H_2O)_2][Cu(Me_4en)]_6\}(ClO_4)_6$ while they cover the range 65.0(6)–79.6(6)° for $\{[Cu_3(mpta)_2(H_2O)_2][Cu(Me_5dien)]_6\}(ClO_4)_6 \cdot 9H_2O$. The average α values of 58.2(5) and 73.8(6)° respectively, exhibit larger deviations from 90° than that found in $K_6[Cu_3(mpta)_3] \cdot 11H_2O$ [average α value of 83.8(7)°]. Hence, the whole nonanuclear units in $\{[Cu_3(mpta)_2(H_2O)_2][Cu(Me_4en)]_6\}(ClO_4)_6$ and

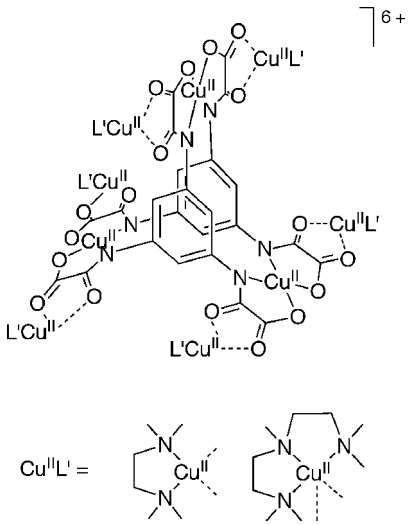

Scheme 11 Structural formula of the homometallic nonanuclear $M^{II}_3M'^{II}_6$ complexes (M = M′ = Cu).

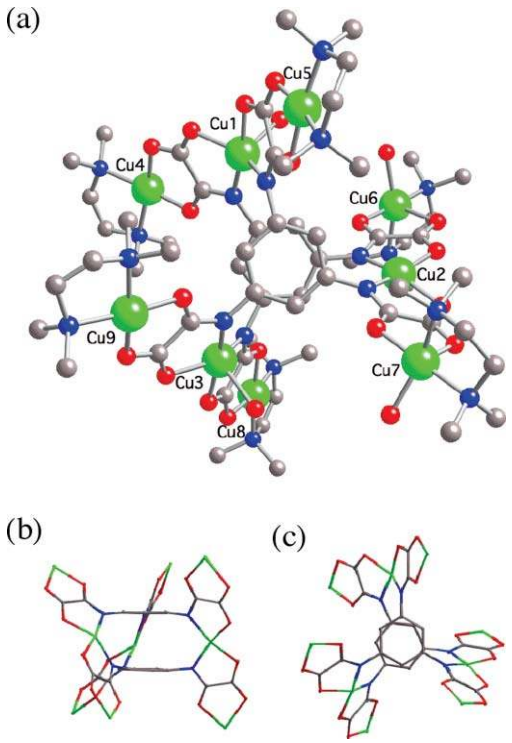

Fig. 19 (a) Perspective view of the cationic nonanuclear unit of $\{[Cu_3(mpta)_2(H_2O)_2][Cu(Me_4en)]_6\}(ClO_4)_6$ with the atom labelling of the metal atoms (hydrogen atoms are omitted for clarity). (b) Side and (c) top views of the octanuclear skeleton standing out the trinuclear metallacyclophane core. See Fig. 1 for color coding.

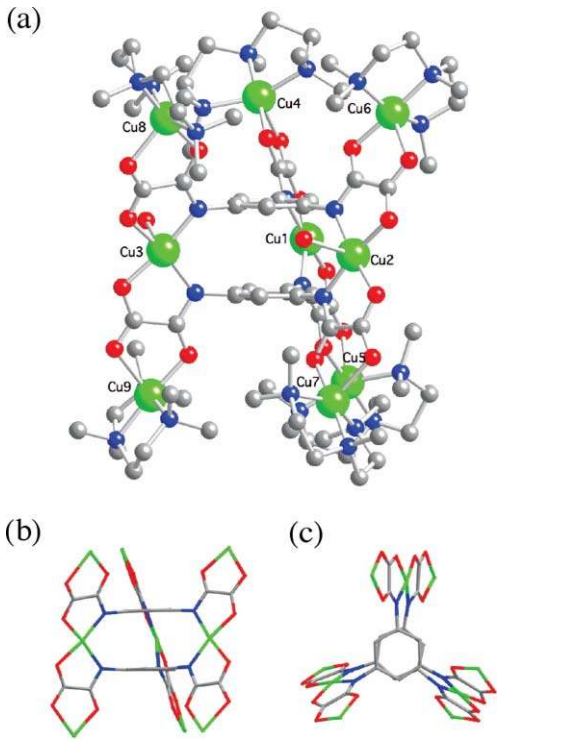

Fig. 20 (a) Perspective view of the cationic nonanuclear unit of $\{[Cu_3(mpta)_2(H_2O)_2][Cu(Me_5dien)]_6\}(ClO_4)_6\cdot 9H_2O$ with the atom labelling of the metal atoms (hydrogen atoms are omitted for clarity). (b) Side and (c) top views of the octanuclear skeleton standing out the trinuclear metallacyclophane core. See Fig. 1 for color coding.

$\{[Cu_3(mpta)_2(H_2O)_2][Cu(Me_5dien)]_6\}(ClO_4)_6\cdot 9H_2O$ have a propeller structure of pseudo D_{3d} molecular symmetry which is chiral, both enantiomers (Δ and Λ) being present in the solid state. Otherwise, the perfect face-to-face alignment of the two benzene rings around the three-fold molecular axis would lead to an achiral nonanuclear complex with a C_{3h} molecular symmetry. All six peripheral copper atoms in $\{[Cu_3(mpta)_2(H_2O)_2]$-$[Cu(Me_5dien)]_6\}(ClO_4)_6\cdot 9H_2O$ adopt a noncoplanar disposition between the Me_5dien ligand and the oxamato group; they are, however, not equivalent in $\{[Cu_3(mpta)_2(H_2O)_2][Cu(Me_4en)]_6\}(ClO_4)_6$ because of the occurrence of both coplanar (Cu4, Cu5, Cu8 and Cu9) and noncoplanar (Cu6 and Cu7) dispositions of the Me_4en ligand and the oxamato group. The average value of the intramolecular distance between the central copper atoms through the double 1,3,5-phenylenetriamidate bridge is 6.779(5) Å for $\{[Cu_3(mpta)_2(H_2O)_2][Cu(Me_4en)]_6\}(ClO_4)_6$ and 6.929(5) Å for $\{[Cu_3(mpta)_2(H_2O)_2][Cu(Me_5dien)]_6\}(ClO_4)_6\cdot 9H_2O$, while the average values of the intramolecular distance between the central and peripheral copper atoms through the oxamato bridge are 5.250(5) and 5.340(5) Å, respectively.

The magnetic properties of this series of oxamato-bridged, homometallic $M^{II}{}_3M'^{II}{}_6$ complexes (M = M′ = Cu) with trinuclear metallacyclophane cores are consistent with a weak ferromagnetic coupling [J' = +7.9 (L′ = Me_4en) and +7.8 cm^{-1} (L′ = Me_5dien)] between the three moderate to strong antiferromagnetically-coupled $Cu^{II}{}_3$ units [J = −318 (L′ = Me_4en) and −106 cm^{-1} (L′ = Me_5dien)] ("trimer-of-trimers" model) [$H = -J(S_{1A}\cdot S_{4A} + S_{1A}\cdot S_{5A} + S_{2B}\cdot S_{6B} + S_{2B}\cdot S_{7B} + S_{3C}\cdot S_{8C} + S_{3C}\cdot S_{9C}) - J'(S_{1A}\cdot S_{2B} + S_{1A}\cdot S_{3C} + S_{2B}\cdot S_{3C})$ with $S_{1A} = S_{2B} = S_{3C} = S_M$ and $S_{4A} = S_{5A} = S_{6B} = S_{7B} = S_{8C} = S_{9C} = S_{M'}$] [Scheme 12(a)].[28a,37] The values of the intratrimer coupling parameter agree with those reported for related oxamato-bridged linear tricopper(II) complexes ($-J$ = 89–357 cm^{-1}).[25l,m,r] The attenuation of the antiferromagnetic coupling through the oxamato bridge caused by the substitution of a bidentate diamine (L′ = Me_4en) by a tridentate triamine (L′ = Me_5dien) as terminal ligand stems from the noncoplanarity of the basal planes of the central and peripheral Cu^{II} ions. On the other hand, the values of the intertrimer coupling parameter agree both in sign and magnitude with that found in the tricopper(II) complex $K_6[Cu_3(mpta)_2]\cdot 11H_2O$ (J' = +11.8 cm^{-1}). The slight decrease of the ferromagnetic coupling through the double 1,3,5-phenylenetriamidate bridge in the nonacopper(II) complexes likely originates from the greater helical torsion of the trinuclear metallacyclophane core.

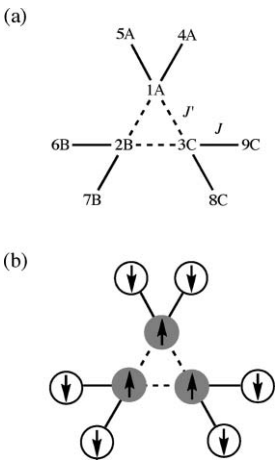

Scheme 12 (a) Spin coupling pattern and (b) spin topology for the nonanuclear $M^{II}{}_3M'^{II}{}_6$ complexes (M = M′ = Cu) with $J < 0$ and $J' > 0$.

Similarly to $Cu^{II}{}_2$ (L = mpba), the $Cu^{II}{}_3$ (L = mpta) metallacyclophane core acts as a "robust" FC unit between the three $Cu^{II}{}_3$ linear fragments ($S_A = S_B = S_C = 2S_{Cu} - S_{Cu} = 1/2$), leading to a quartet ground spin state for the $Cu^{II}{}_9$ complexes ($S = S_A + S_B + S_C = 3/2$) [Scheme 12(b)]. To extend these promising results, we aim at using this trinuclear copper(II) metallacyclophane as ligand toward other M'^{II} (M = Ni, Co and Mn) ions, in order to get heterometallic nonanuclear complexes with larger values of the spin and magnetic anisotropy as potential candidates to high-T_B SMMs. These high-spin molecules would benefit from the moderately strong antiferromagnetic coupling between the M^{II} and M'^{II} ions through the oxamato bridge and the moderately weak ferromagnetic coupling between the M^{II} ions across the 1,3,5-substituted benzenetriyl spacers; however, they are severely limited by the relatively high molecular symmetry which leads to low values of the magnetic anisotropy and consequently, to small activation energy barriers.

*n*D Coordination polymers (*n* = 1–3)

One-dimensional compounds

The mononuclear copper(II) complexes $[Cu^{II}L_2]^{2-}$ (L = pmaMe, $pmaMe_2$ and $pmaMe_3$) act as bis(bidentate) ligands toward fully solvated M'^{II} ions (M = Mn and Co) in either dimethyl sulfoxide or water to afford neutral heterobimetallic one-dimensional compounds of general formula $[M'^{II}Cu^{II}L_2S_2]_n$ (S = dmso or H_2O) [Scheme 4(a)].[28b] The crystal structures of $CoCu(pmaMe_2)_2(H_2O)_2$ and $CoCu(pmaMe_3)_2(H_2O)_2\cdot 4H_2O$ show either zigzag or linear 1D architectures according to whether the two solvent molecules are coordinated to the octahedral Co^{II} ions in *cis* or *trans* positions, respectively [Fig. 21(a) and 22(a)].[29] In the former case, the regular alternating of enantiomers of opposite propeller chirality (Δ and Λ) for the *cis*-diaqua Co^{II} ions leads to the overal achiral zigzag chain structure, instead of the chiral helical chain (right- or left-handed) that would result in the case of enantiomers of identical chirality (Δ or Λ).[29b]

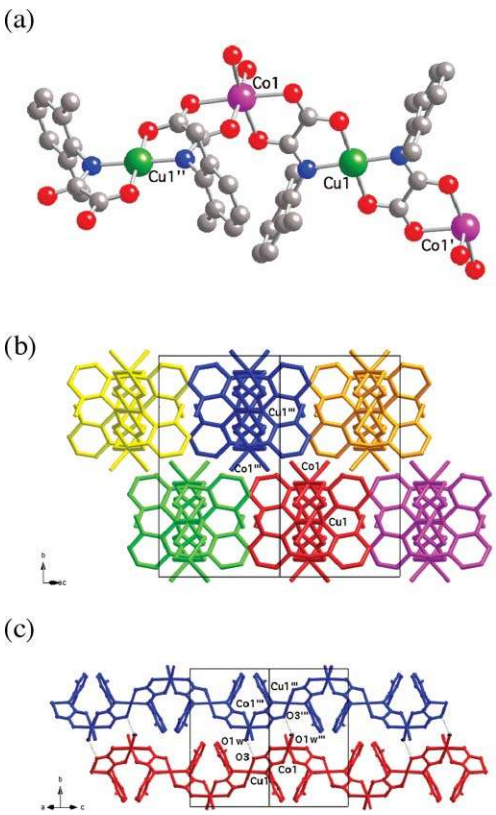

Fig. 21 (a) Perspective view of a fragment of the zigzag chain of $CoCu(pmaMe_2)_2(H_2O)_2$ with the atom labelling of the metal atoms (hydrogen atoms are omitted for clarity). (b) and (c) Drawings of the crystal packing of the chains along the [10$\bar{1}$] and [101] directions, respectively (hydrogen bonds are represented by dashed lines) [symmetry codes: (I) = $1/2 - x, 1/2 - y, -z$; (II) = $-x, y, 1/2 - z$; (III) = $x, 1 - y, 1 - z$]. See Fig. 1 for color coding.

In both compounds, the neutral oxamato-bridged $Co^{II}Cu^{II}$ chains are rather well separated from each other in the crystal lattice due to the presence of the bulky methyl-substituted phenyl groups which are almost perpendicular to the oxamato bridges [Fig. 21(b) and 22(b)]. However, there are weak interchain hydrogen bonds involving the coordinated water molecules and either the carbonyl-oxygen atoms from the oxamato bridging groups in $CoCu(pmaMe_2)_2(H_2O)_2$ or the crystallization water molecules in $CoCu(pmaMe_3)_2(H_2O)_2\cdot 4H_2O$ [Fig. 21(c) and 22(c)]. The values of the intrachain Cu–Co distance through the oxamato bridge for $CoCu(pmaMe_2)_2(H_2O)_2$ and $CoCu(pmaMe_3)_2(H_2O)_2\cdot 4H_2O$ are 5.296(1) and 5.301(2) Å respectively, while the shortest interchain Co–Co separations through these one- or three-water hydrogen-bonded motifs are 5.995(5) and 8.702(3) Å.

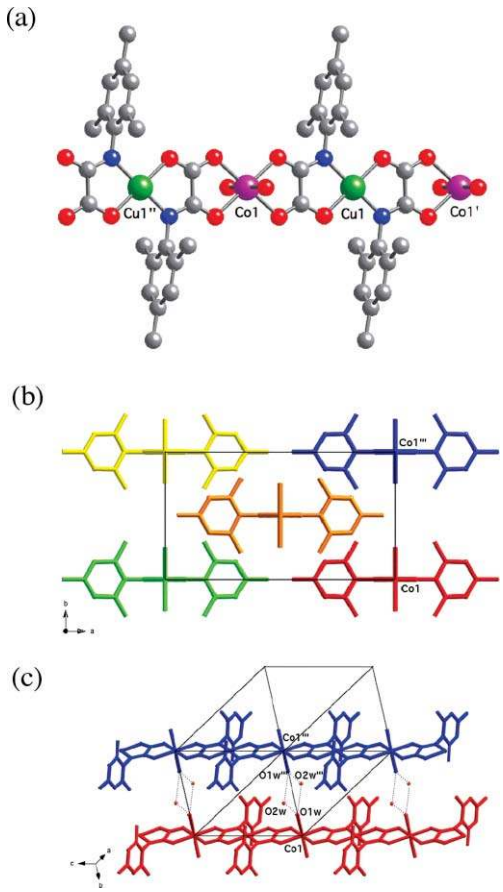

Fig. 22 (a) Perspective view of a fragment of the linear chain of $CoCu(pmaMe_3)_2(H_2O)_2\cdot 4H_2O$ with the atom labelling of the metal atoms (hydrogen atoms are omitted for clarity). (b) and (c) Drawings of the crystal packing of the chains along the [001] and [111] directions, respectively (hydrogen bonds are represented by dashed lines) [symmetry codes: (I) = $-x, y, -z$; (II) = $-x, y, 1 - z$; (III) = $x, 1 + y, z$]. See Fig. 1 for color coding.

The series of $M'^{II}Cu^{II}$ chain compounds (M′ = Mn and Co) with sterically-hindered polymethyl-substituted phenyloxamato ligands (L = pmaMe, $pmaMe_2$ and $pmaMe_3$) behave as almost ideal 1D ferrimagnets.[29] In all the cases, the moderately strong antiferromagnetic coupling between the M'^{II} and the Cu^{II} ions through the oxamato bridge is large enough to allow a short-range intrachain magnetic correlation [$-J$ = 24.7–27.9 (M′ = Mn) and 35.0–45.8 cm^{-1} (M′ = Co)] [$H = \sum_{i=1-n} -J(S_{2i}\cdot S_{2i-1})$ with $S_{2i} = S_{M'}$ and $S_{2i-1} = S_{Cu}$], as previously found for related oxamato-bridged manganese(II)–copper(II) and cobalt(II)–copper(II) chains.[26] However, only the $Co^{II}Cu^{II}$ chains exhibit slow magnetic relaxation effects at low temperatures (T_B < 3.5 K) typical of SCMs, more likely because of the large values of the axial magnetic anisotropy

of the Co^{II} ion (D = 538–719 cm^{-1}) [$H = \sum_{i=1-n}\{-J(S_{2i}\cdot S_{2i-1}) - a\lambda(L_{z2i}\cdot S_{z2i}) + DL_{z2i}^2\}$ with $S_{2i} = S_{Co}$ and $S_{2i-1} = S_{Cu}$].[29b]

The analysis of the temperature dependence of the relaxation time for $CoCu(pmaMe_3)_2(dmso)_2\cdot dmso$ and $CoCu(pmaMe_3)_2(H_2O)_2\cdot 4H_2O$ shows a thermally-activated mechanism for the magnetic relaxation as $\tau = \tau_0 \exp(E_a/k_BT)$ (Arrhenius law's dependence) (Fig. 23).[29b] The values of E_a are 38.0 (S = dmso) and 16.3 cm^{-1} (S = H_2O), while those of τ_0 are 2.3×10^{-11} (S = dmso) and 4.0×10^{-9} s (S = H_2O). They all lie in the range of those previously reported for other SCMs.[21] The greater the values of the antiferromagnetic intrachain coupling [$-J$ = 44.3 (S = dmso) and 35.0 cm^{-1} (S = H_2O)] and the axial magnetic anisotropy [D = 710 (S = dmso) and 610 cm^{-1} (S = H_2O)] are, the higher the activation energy for magnetization reversal is, as observed.[29b] In fact, the activation energy for a ferrimagnetic chain on the basis of the Glauber's theory for an Ising one-dimensional system depends on the intrachain coupling constant (J) and the axial magnetic anisotropy (D) according to the expression $E_a = (4|J| + |D|)S^2$.[21]

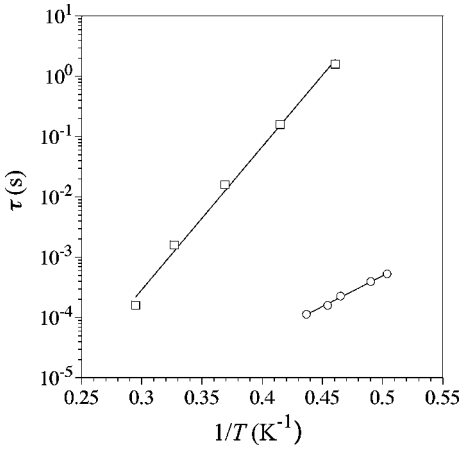

Fig. 23 Arrhenius plot for $CoCu(pmaMe_3)_2(dmso)_2\cdot dmso$ (□) and $CoCu(pmaMe_3)_2(H_2O)\cdot 4H_2O$ (○) (the solid lines are the best-fit curves).

This unprecedented SCM behavior for the family of oxamato-bridged, heterobimetallic $Co^{II}Cu^{II}$ chains obeys to the large intrachain Ising-type magnetic anisotropy and to the minimization of the interchain interactions which result from the combination of an orbitally degenerate octahedral high-spin Co^{II} ion ($^4T_1$) and a square-planar Cu^{II} complex with bulky methyl-substituted phenyl groups, respectively. As a matter of fact, the values of the blocking temperature along this series follow the steric hindrance of both the aromatic group-substituted oxamato ligand (pmaMe < $pmaMe_2$ < $pmaMe_3$) and the coordinated solvent molecule (H_2O < dmso). We are currently searching for new mononuclear copper(II) precursors with long alkyl- or aryl-group substituted phenyloxamate ligands of even larger steric hindrances in order to obtain well isolated oxamato-bridged heterobimetallic chains as potential candidates to high-T_B SCMs.

Two-dimensional compounds

The dicopper(II) complexes $[Cu^{II}_2L_2]^{4-}$ (L = mpba and $mpbaMe_3$) act as tetrakis(bidentate) ligands toward fully solvated Co^{II} ions in water, affording neutral heterobimetallic two-dimensional compounds of general formula $[Co^{II}_2Cu^{II}_2L_2(H_2O)_6]_n$ [Scheme 4(c)].[28c] The crystal structure of $Co_2Cu_2(mpba)_2(H_2O)_6\cdot 6H_2O$ shows a 'brick-wall' 2D architecture of (6,3) net topology (the first symbol in the Wells' notation indicates the number of nodes of the smallest closed circuit in the net while the second one is the number of connections radiating from each node to the neighboring ones) (Fig. 24).[35] Within each rectangular cell unit, there are six square-pyramidal Cu^{II} ions with an axially coordinated water molecule which occupy the four corners and the middle point of the two long edges of the rectangle, and four octahedral Co^{II} ions with two *trans*-coordinated water molecules which sit at one-fourth- and three-fourth-point of each long edge [Fig. 24(a)]. Each $Co^{II}_2Cu^{II}_2$ rectangular layer is made up of oxamato-bridged $Co^{II}Cu^{II}$ linear chains running parallel to the a axis which are further connected through two *m*-phenylenediamidate bridges between the Cu^{II} ions to give dinuclear metallacyclic cores of the cyclophane-type which define the short edge of the rectangle [Fig. 24(b)]. The neighboring chains form a dihedral 'bite' angle of 121.5° because of the *meta* topology of the phenylene spacer, conferring the planes with a global corrugated shape [Fig. 24(c)]. The Cu–Co distance through the oxamato bridge is 5.342(5) Å, whereas the Cu–Cu separation through the double *m*-phenylenediamidate bridge is 6.398(5) Å.

The adjacent corrugated layers in the crystal lattice closely stack above each other to give an infinite array of interdigitated (not interpenetrated) layers along the b axis [Fig. 24(c)]. Weak hydrogen bonds involving the coordinated water molecules and the carbonyl-oxygen atoms from the oxamato bridging groups of adjacent layers occur, as previously observed for the parent chain compound $CoCu(pmaMe_2)_2(H_2O)_2$. Because of this zipper-type packing, the shortest metal-metal interlayer separations involve ions of the same nature. The shortest interlayer Co–Co distance through this hydrogen-bonded motif is 4.848(5) Å. These neighboring layers are displaced in a parallel manner along the a axis, so that their internal rectangular cavities are not aligned leading thus to small square pores which are occupied by hydrogen-bonded crystallization water molecules [Fig. 24(d)].

In this series of metallacyclophane-based $Co^{II}_2Cu^{II}_2$ layered compounds with *m*-phenylenebis(oxamato) ligands (L = mpba and $mpbaMe_3$), the double *meta*-substituted phenylene linkers ensure a ferromagnetic interaction between the oxamato-bridged ferrimagnetic chains. Hence, complex $Co_2Cu_2(mpba)_2(H_2O)_6\cdot 6H_2O$ is a metamagnet with a long-range 3D antiferromagnetic ordering in zero-field at T_N = 8.5 K and a ferromagnetic-like transition at a critical field of 1.2 kOe which is sufficient to overcome the weak interlayer antiferromagnetic interactions.[35] This metamagnetic behavior is confirmed by the sigmoidal shape of the magnetization isotherm at 2.0 K with a characteristic inflexion point occurring at an applied field around 1.2 kOe which is followed by the aperture of a narrow magnetic hysteresis loop characteristic of soft magnets (Fig. 25).[35]

In contrast, complex $Co_2Cu_2(mpbaMe_3)_2(H_2O)_6\cdot 6H_2O$ shows a long-range (most likely 2D) ferromagnetic order at T_C = 24.0 K because of the minimization of the interlayer magnetic interactions that would lead to well isolated planes of Ising-type magnetic anisotropy.[28c] That being so, the differences in the magnetic ordering of $Co_2Cu_2(mpba)_2(H_2O)_6\cdot 6H_2O$ and $Co_2Cu_2(mpbaMe_3)_2(H_2O)_6\cdot 6H_2O$ are attributed to the presence of the methyl substituents on the phenylenedioxamato ligands which keep away the planes from each other, weakening the

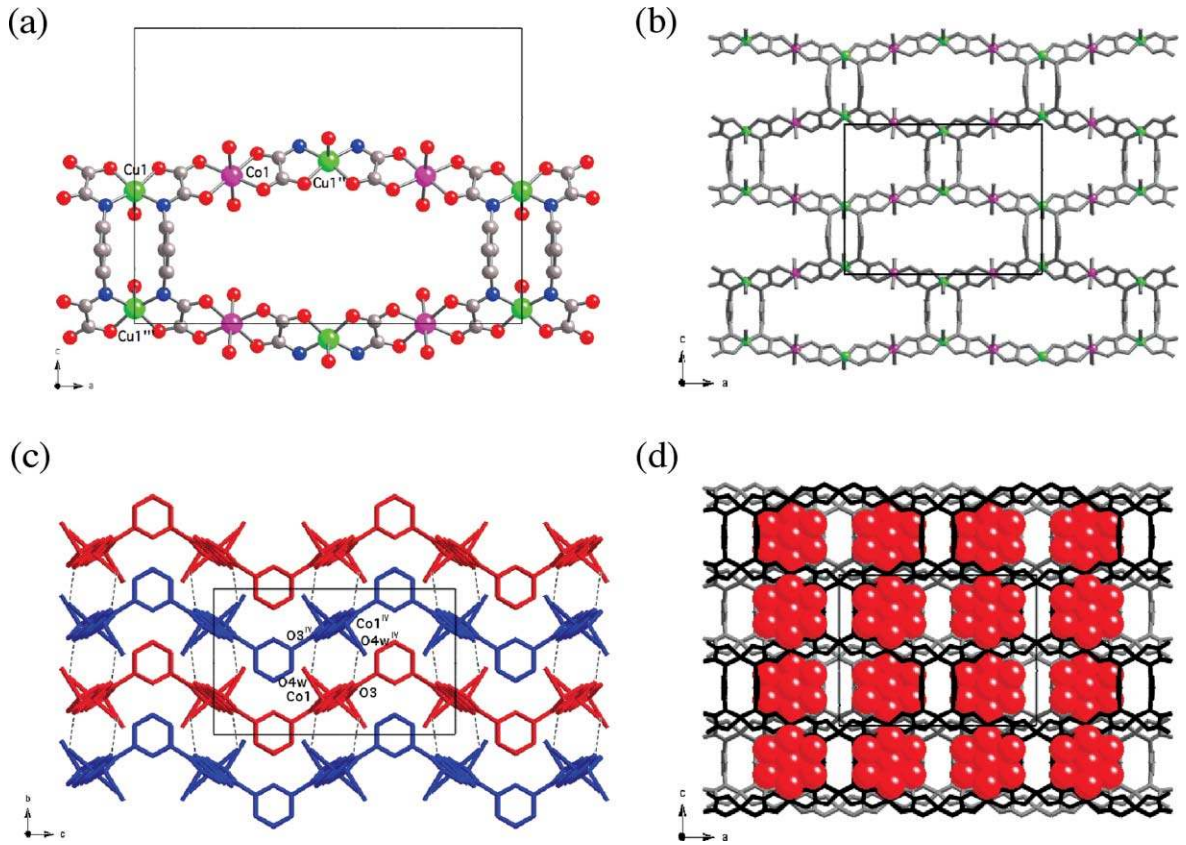

Fig. 24 (a) Perspective view of a rectangular cell of $Co_2Cu_2(mpba)_2(H_2O)_6{\cdot}6H_2O$ with the atom labelling of the metal atoms (hydrogen atoms are omitted for clarity) [symmetry codes: (I) = $-x, y, z$; (II) = $-x, -y, -z$; (III) = $-x, y, -z$; (IV) = $x, -y, -z$]. (b) and (c) Projection views of the 'brick-wall' network along the *b* and *a* axes, respectively (hydrogen bonds are represented by dashed lines). (d) Drawing of the crystal packing along the *b* axis showing the filling of the square pores of the open-framework structure by crystallization water molecules (oxygen atoms are represented by red spheres). See Fig. 1 for color coding.

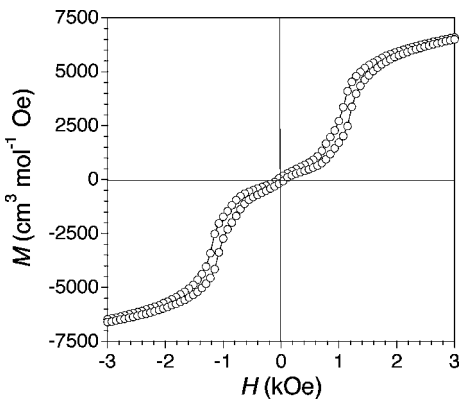

Fig. 25 Magnetization hysteresis loop for $Co_2Cu_2(mpba)_2(H_2O)_6{\cdot}6H_2O$ at 2.0 K.

interlayer interactions (dipolar and/or hydrogen bonding). These two examples clearly illustrate the strong influence of the interplanar interactions on the magnetic ordering in bimetallic layered compounds. A ferromagnetic ordering occurs when the interlayer separation is large, the antiferromagnetic interplanar interactions being negligible. Metamagnetism appears, instead, when the interlayer separation is small enough to make possible the occurrence of antiferromagnetic interplanar interactions.

In addition, slow magnetic relaxation effects at T_B *ca.* 5.0 K are observed in the antiferromagnetic ordered state for $Co_2Cu_2(mpba)_2(H_2O)_6{\cdot}6H_2O$.[35] These effects can be attributed to the formation of small magnetic domains of strongly correlated spins within the weakly interacting oxamato-bridged ferrimagnetic chains. However, the dynamics of the magnetization relaxation is different from that of the cobalt(II)–copper(II) chain analogues described above, but it is more typical of spin glasses.[42a] We are currently searching for new dinuclear copper(II) precursors with longer oligophenylene spacers in order to obtain $Co^{II}_2Cu^{II}_2$ layered compounds with rather well-isolated oxamato-bridged ferrimagnetic chains which would allow us to investigate the origin of this low-temperature glassy behavior.

Three-dimensional compounds

The dinickel(II) and dicobalt(II) complexes $[M^{II}_2L_3]^{8-}$ (M = Ni and Co; L = mpba) act as hexakis(bidentate) ligands toward either fully solvated M'^{I} (M' = Li) or M'^{II} (M' = Mn) ions in water to give anionic heterobimetallic three-dimensional compounds of general formula $[M'^{I}_3M^{II}_2L_3(H_2O)_6]_n^{5n-}$ and $[M'^{II}_3M^{II}_2L_3(H_2O)_6]_n^{2n-}$, respectively [Scheme 4(d)].[28b] The crystal structures of the lithium salts $Li_5[Li_3M_2(mpba)_3(H_2O)_6]{\cdot}31H_2O$ (M = Ni and Co) show a 3D 'honeycomb' architecture of (6,4) net topology (Fig. 26).[36] Within each hexagonal prismatic cell unit, there are twelve and ten

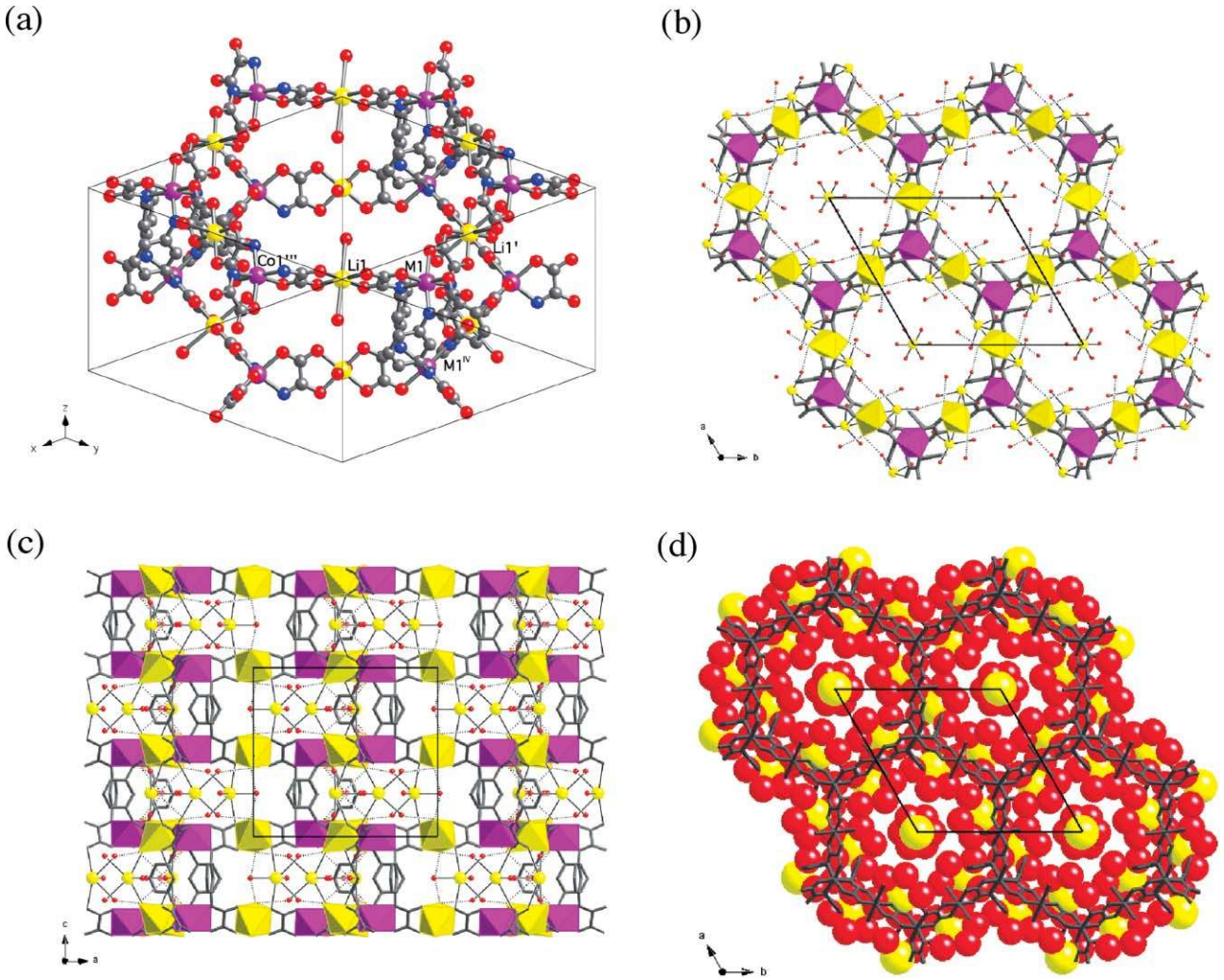

Fig. 26 (a) Perspective view of a hexagonal prismatic cell of $Li_5[Li_3M_2(mpba)_3(H_2O)_6]\cdot 31H_2O$ (M = Ni and Co) with the atom labelling of the metal atoms (hydrogen atoms are omitted for clarity) [symmetry codes: (I) = $-y$, $x - y$, z; (II) = $-x + y$, $-x$, z; (III) = $-x$, $-y$, $-z$; (IV) = x, y, $1/2 - z$]. (b) and (c) Projection views of the 'honeycomb' network along the *c* and *b* axes, respectively (weak interactions with the lithium counter-cations and hydrogen bonds with the coordinated water molecules are represented by solid and dotted lines, respectively). (d) Drawing of the crystal packing along the *c* axis showing the filling of the hexagonal pores of the open-framework structure by solvated lithium counter-cations and crystallization water molecules (lithium and oxygen atoms are represented by yellow and red spheres, respectively). See Fig. 1 for color coding.

metal sites per each hexagonal and rectangular face respectively: six octahedral M^{II} ions (M = Ni and Co) of opposite propeller chirality (Δ and Λ) regularly alternate in the corners of each hexagon or in the four corners and the middle point of the two long edges of each rectangle, whereas either six or four octahedral Li^{I} ions with two *trans*-coordinated water molecules sit at the middle of each edge of the hexagon or at the one-fourth- and three-fourth-point of each long edge of the rectangle, respectively [Fig. 26(a)].

The crystal lattice of these two isostructural compounds consists of an infinite parallel array of anionic oxamato-bridged $Li^{I}{}_3M^{II}{}_2$ hexagonal layers growing in the *ab* plane [Fig. 26(b)]; the adjacent layers are interconnected through three *m*-phenylenediamidate bridges between the M^{II} ions of opposite propeller chirality (Δ and Λ) to give dinuclear metallacryptand cores of the *meso*-helicate-type which act as pillars of the hexagonal prismatic structure [Fig. 26(c)]. The values of the Li–M distance through the oxamato bridge are 5.380(5) (M = Ni) and 5.396(5) Å (M = Co), while those of the M–M separation through the triple *m*-phenylenediamidate bridge are 6.856(5) (M = Ni) and 6.851(3) Å (M = Co). Overall, this leads to an open-framework with large hexagonal pores along the *c* axis of 21.8 (M = Ni) and 21.5 Å (M = Co) in diameter [defined as the M–M distance between directly opposed metal atoms in the hexagon] and small rectangular pores along the *b* axis of dimensions 6.9 × 18.6 (M = Ni) and 6.9 × 18.7 Å (M = Co) [defined as the M–M distances between the metal atoms occupying the corners of the short and long edges in the rectangle, respectively]. These pores are occupied by either weakly coordinated or noncoordinated solvated Li^{I} countercations, together with a significant amount of hydrogen-bonded crystallization water molecules [Fig. 26(d)].

The magnetic properties of this family of metallacryptand-based M'_3M_2 open-framework compounds ($M' = Li^{I}$ and Mn^{II}; $M = Ni^{II}$ and Co^{II}) with the *m*-phenylenebis(oxamate) ligand (L = mpba) depend mainly on the diamagnetic or

paramagnetic nature of M′ and on the magnetic anisotropy of M.[36] Hence, the compounds $Li_5[Li_3M_2(mpba)_3(H_2O)_6]\cdot 31H_2O$ (M = Ni and Co) behave as well-isolated M^{II}_2 complexes with a weak ferromagnetic interaction between the M^{II} ions (M = Ni and Co) across the three *meta*-substituted phenylenediamidate bridges within the metallacryptand core [J = +3.2 (M = Ni) and +1.0 cm^{-1} (M = Co)], as for the aforementioned sodium derivatives $Na_4[M_2(mpba)_3]\cdot 12H_2O$ [J = +3.6 (M = Ni) and +1.3 cm^{-1} (M = Co)]; the next nearest-neighbor magnetic interactions between the M^{II} ions (M = Ni and Co) through the coordinated Li^{I} ions are negligible. Similarly, the three *meta*-substituted phenylene linkers ensure a ferromagnetic interaction between the oxamato-bridged ferrimagnetic planes in the compounds $Li_2[Mn_3M_2(mpba)_3(H_2O)_6]\cdot 22H_2O$ (M = Ni and Co), which leads to a long-range 3D ferromagnetic order at T_C = 6.5 K for both of them. Indeed, the ferromagnetic nature of the transition is confirmed by the magnetic hysteresis loops at 2.0 K (Fig. 27), which are characteristic of soft magnets as evidenced by the relatively low values of the coercive field [H_c = 450 (M = Ni) and 175 Oe (M = Co)] and the remnant magnetization [M_r = 8930 (M = Ni) and 1205 $cm^3\ mol^{-1}$ Oe (M = Co)]. The lower values of H_c and M_r for $Li_2[Mn_3Co_2(mpba)_3(H_2O)_6]\cdot 22H_2O$ when compared to those of $Li_2[Mn_3Ni_2(mpba)_3(H_2O)_6]\cdot 22H_2O$ seems surprising because of the greater magnetic anisotropy of the octahedral high-spin Co^{II} ion against that of the Ni^{II} one with $^4T_1$ and $^3E_1$ ground states, respectively. In fact, the coercivity is not an intrinsic phenomenon but also depends on a number of extrinsic factors such as the crystallinity and the grain size of the sample.

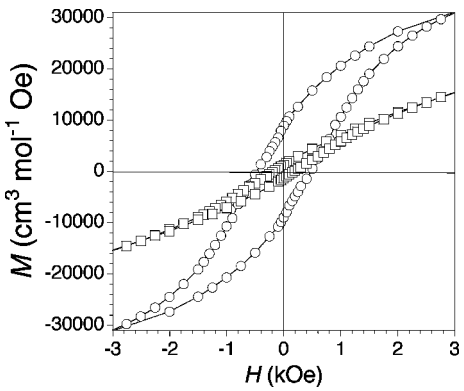

Fig. 27 Magnetization hysteresis loops for $Li_2[Mn_3Ni_2(mpba)_3(H_2O)_6]\cdot 22H_2O$ (○) and for $Li_2[Mn_3Co_2(mpba)_3(H_2O)_6]\cdot 22H_2O$ (□) at 2.0 K (the solid lines are eye-guides).

The family of $M'^{II}_3M^{II}_2$ open-framework compounds (M′ = Mn; M = Ni and Co) affords the first examples of oxamato-bridged heterobimetallic 3D molecule-based magnets. Although they are severely limited by the low values of the magnetic ordering temperature (T_C = 6.5 K) and coercivity (H_c = 175–450 Oe), their structure makes them very appealing candidates as porous magnets and host–guest magnetic sensors.[43] On the other hand, the substitution of the alkaline inorganic counter-cations in the anionic 3D host framework by other cationic guest molecules, reaching from organic to organometallic radicals either conducting or magnetic like tetrathiofulvalenes and metallocenes respectively, opens excellent perspectives in multifunctional materials chemistry.[18] In addition, they show unique magnetic relaxation dynamics characteristic of spin glasses, as recently observed in a related oxamato-bridged cobalt(II)–copper(II) compound with a 2D honeycomb structure.[27n] This glassy behavior is most likely attributed to their amorphous character; however, the moderate to strong magnetic anisotropy of the dinickel(II) and dicobalt(II) precursors cannot be neglected. We are currently searching for related mononuclear nickel(II) and cobalt(II) precursors with sterically-hindered polymethyl-substituted phenyloxamate ligands (L = pma, pmaMe, $pmaMe_2$ and $pmaMe_3$) in order to get well isolated $M'^{II}_3M^{II}_2$ (M = Ni and Co; M′ = Co and Mn) ferrimagnetic planes [Scheme 4(b)], which would allow us to investigate the origin of the low-temperature glassy behavior observed in their parent 3D analogues.

Conclusions and outlook: from supramolecular magnetism to supramolecular electronics and nanotechnology

Toward magnetic molecular devices through exchange-coupled metallosupramolecular complexes

The design and synthesis of ligands that are able to self-assemble spontaneously with paramagnetic metal ions to form exchange-coupled metallosupramolecular complexes of predetermined nuclearity and topology are one of the major goals in supramolecular magnetism. Our strategy in this field has been based on the use of polytopic ligands possessing multiple oxamato donor groups, separated by more or less hindered, polymethyl-substituted aromatic benzene spacers of varying substitution pattern. These aromatic polyoxamato (APOXA) ligands coordinate to the late first-row transition metal ions, from copper to cobalt, to afford stable oligonuclear metallacyclic complexes. Overall, we have shown that aromatic benzene spacers are really effective to transmit exchange interactions between paramagnetic metal centers separated by relatively long intermetallic distances in discrete metallacyclic entities. Furthermore, we have demonstrated that the appropriate choice of the electronic configuration of the metal ion and the topology of the bridging ligand allows to control the nature and magnitude of the magnetic coupling between the metal centers through the aromatic benzene spacers in the corresponding di- and trinuclear metallacyclic complexes.

The development of this unique series of oligonuclear exchange-coupled metallosupramolecular complexes with APOXA ligands and late 3d metal ions has provided deeper insights on the fundamental knowledge of the distinct spin-delocalization and spin-polarization effects which govern the magnetic coupling through extended π-conjugated aromatic phenylene bridges. This has directed our current research efforts toward other dicopper(II) and tricopper(II) metallacyclophane molecules with extended π-conjugated aromatic spacers such as linear oligophenylenes (OPs) and oligoacenes (OAs) on one hand,[30b,c] or C_3-symmetrical oligo(phenylenevinylenes) (OPVs) and oligo(phenyleneethynylenes) (OPEs) on the other hand [Scheme 13(a) and (b)]. At this respect, the large oligoacenes (beyond pentacene) are very appealing candidates as molecular wires because of their unique electronic properties which have received much attention from both experimental and theoretical points of view.[44] As a matter of fact, the design and synthesis

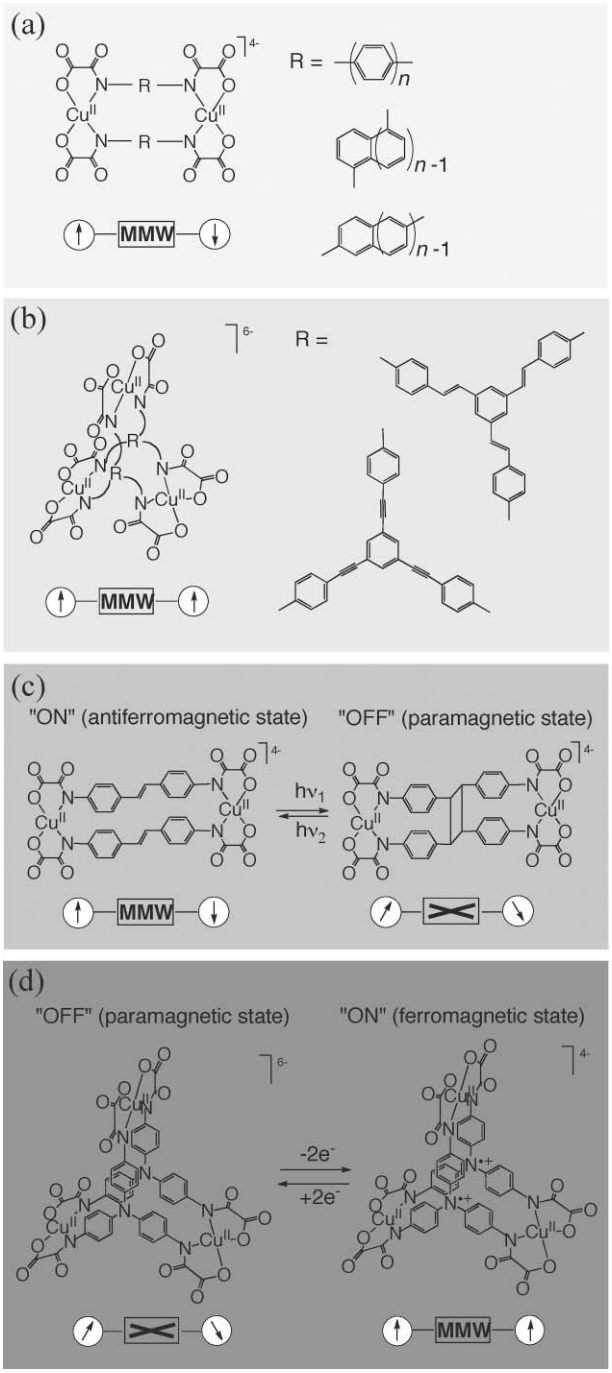

Scheme 13 Proposed models for magnetic molecular devices based on exchange-coupled di- and trinuclear copper(II) metallacyclophanes with APOXA ligands: (a) antiferro- and (b) ferromagnetically-coupled molecular wires, and (c) photo- and (d) redox-active, antiferro- and ferromagnetically-coupled molecular switches.

of novel bridging ligands that can act as effective molecular wires to transmit spin coupling effects over long distances are a major achievement in the field of supramolecular magnetism.[12] In contrast to conventional charge transport-based molecular wires, these so-called "magnetic molecular wires" (MMWs) may offer a new design concept for the transfer of information over long distances based on purely electron exchange interactions and without current flow.

The next step in our ligand design approach to exchange-coupled metallosupramolecular complexes with APOXA ligands will be the incorporation of photo- or electro-active aromatic spacers in the dicopper(II) and tricopper(II) metallacyclophane molecules [Scheme 13(c) and (d)]. At this respect, diarylethenes (stilbene) and triarylamines (triphenylamine) spacers are very appealing candidates as "magnetic molecular switches" (MMSs) because of their unique photochromic and redox properties, respectively.[45,46] These target molecules present two metastable states ('ON/OFF') which can be reached in a reversible manner through photo- or electrochemical processes and which have totally different magnetic properties. The spins of the magnetic centers are ferro- or antiferromagnetically coupled in one of the states ('ON'), whereas they are magnetically isolated in the other one ('OFF'). In the first example, the 'ON/OFF' process is a reversible photochemical reaction between the two facing stilbene spacers. This gives the corresponding [2 + 2] addition product which lacks the π-conjugated character present in the diarylethene precursor [Scheme 13(c)]. The one-electron oxidation of the nonconjugated triphenylamine spacers to afford the corresponding partly delocalized triphenylaminium radicals plays the role of the 'ON/OFF' process in the second example [Scheme 13(d)]. This new family of photo- and redox-active exchange-coupled metallosupramolecular complexes exhibiting a bistable behavior are very promising candidates for nanometer-scale electronic devices in the emerging field of supramolecular electronics.[47]

Toward multifunctional molecular magnets through multidimensional magnetic materials

The design and synthesis of simple paramagnetic molecules that are able to self-assemble through metal–ligand interactions to form more complex aggregates (supermolecules) with prefixed dimensionality, nuclearity, and/or topology is a major target in supramolecular magnetism. Our strategy in this field has been based on the use of oligonuclear oxamato metal complexes, from mono- to trinuclear, as metalloligands toward either coordinatively unsaturated metal complexes or fully solvated transition metal ions affording discrete polynuclear coordination compounds or infinite coordination polymers, respectively. Moreover, this well known "complex-as-ligand" approach allows to control the overall magnetic properties of the resulting *n*D (*n*D = 0–3) multidimensional compound through the appropriate choice of the metalloligand precursor (substitution pattern and steric requirements of the bridging ligand) and the coordinated metal ion or metal complex (electronic configuration and local anisotropy).

The development of this unique family of oxamato-bridged polynuclear coordination compounds, from penta- to nonanuclear, and coordination polymers with APOXA ligands expands on the reported examples of multidimensional magnetic materials build up from related oxamato analogues mentioned in the introduction. This has provided the first examples of SMMs and SCMs within this class and at the same time, allowed the entry to a new class of higher dimensionality molecule-based magnets. Having in mind their applications in material sciences

and nanotechnology, we will focus on self-assembling, multifunctional molecular magnets incorporating properties other than the purely magnetic ones (redox, optical, ferroelectrical, or electrical conduction) on one hand, and on their subsequent addressing into suitable surfaces and other confined media (mesoporous silica, Langmuir–Blodgett films, SAMs, or gold films) on the other hand. These two topics can be achieved from the viewpoint of ligand design by developing a new class of APOXA ligands differently functionalized with photo- or electro-active aromatic substituents; in certain cases, they are either self-assembled in the crystal lattice or bonded to the host surface through electrostatic, hydrophobic, and π–π interactions, or hydrogen and dative bonds (Scheme 14).

The first topic in our ligand design approach to self-assembling, multifunctional molecular magnets would be the preparation of mononuclear copper(II) precursors with either stereogenic or donor group-substituted, homo- or heteroleptic aromatic bis(oxamate) chelating ligands to build up 1D arrays of double heterobimetallic chains [Scheme 14(a) and (b)]. In this regard, chiral binaphthyl and phenanthroline[24d] derivatives are very appealing candidates for the elaboration of optically-active and photoswitching magnetic materials, respectively. In the first example, these so-called chiral magnets may possess novel magnetooptical properties resulting from the interaction between polarized light and the electron spins (magneto-chiral dichroism).[19] In the second example, the additional coordinated metal is photoactive, such as the diamagnetic low-spin Fe^{II} and Ru^{II} ions. Hence, the well-known photoinduced electron transfer in ruthenium(II) polypyridine-type complexes or the recently discovered 'light-induced-excited-state-spin-trapping' (LIESST) effect in spin-crossover iron(II)–polypyridine complexes can be used to modulate the magnetic properties of the individual chains under irradiation.[48,49]

The second topic in our ligand design approach to self-assembling, addressable multifunctional molecular magnets would concern the use of mononuclear copper(II) precursors with either alkoxo- or polyheterocyclic-substituted aromatic monooxamate ligands to build up 2D arrays of heterobimetallic chains [Scheme 14(c) and (d)]. At this respect, long hydrocarbon (dodecyl or hexadecyl) side chains and oligothiophene-based derivatives are very appealing candidates for the elaboration of thermoresponsive and electro-switching magnetic materials respectively, through either 'sol–gel' polymerization in nonpolar solvents or electropolymerization on electrode surfaces. A rich temperature-dependent mesomorphic and magnetic behavior may be associated to the thermally-induced liquid crystalline (LC) phase transition in the first example. This could be modulated by playing with the size of the alkyl chains within the hydrophobic layers. These studies can lead to a new class of multifunctional materials, namely magnetic metallomesogens, which may have novel applications in the field of nanotechnology.[50] In the second example, the partial oxidation of the oligothiophene units within the π–π stacks may confer electron conducting properties. The coexistence of magnetic ordering and electrical conduction in these so-called magnetic molecular conductors is a major target in the field.[18] In fact, the interactions between the itinerant electrons of the conducting stacks and the localized spins in the chains would serve to tune the original magnetic behavior.

In summary, the combined work of our different research teams on the supramolecular coordination chemistry of APOXA ligands with paramagnetic 3d metal ions exemplifies the current trends and the future challenges ('state-of-the-art') in the metallosupramolecular design strategy to magnetic materials. Although still in its infancy, this 'bottom-up' approach appears as an advantageous alternative to the classical 'top-down' one to nanoscopic functional materials displaying unique magnetic

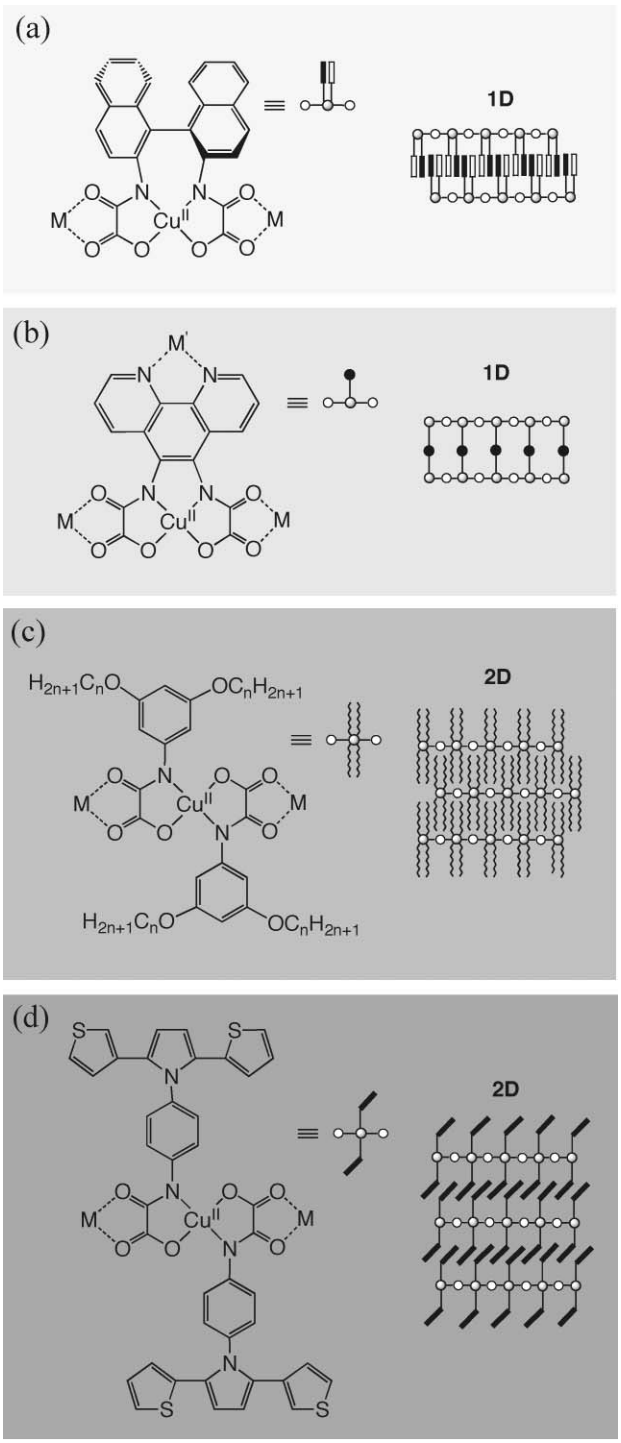

Scheme 14 Proposed models for self-assembling multifunctional molecular materials based on mononuclear copper(II) complexes with APOXA ligands: (a) optically-active and (b) photo-switched 1D molecular magnets, (c) thermo-responsive and (d) redox-switched 2D molecular magnets.

properties as well as redox, optical, conducting, sensor, or catalytic activities.[51] As a matter of fact, the morphosynthesis of novel hybrid materials from the multilevel organization of molecules with interesting chemical and physical properties into suitable ordered host systems is a major current challenge in material science and nanotechnology which requires the collaboration of groups from different disciplines, including organic, inorganic, or theoretical chemists and physicists.[52] Doubtless, this is the more attractive part of this approach and the main reason for us to pursue along this research avenue.

Acknowledgements

This work was supported by the Ministerio de Educación y Ciencia and the Ministerio de Ciencia y Tecnología (MEC and MCyT, Spain) through the Ramón y Cajal program the Consolider-Ingenio in Molecular Nanoscience (Project CSD2007-00010) and the Plan Nacional de Investigación Científica, Desarrollo e Innovación Tecnológica (Projects CTQ2004-03633, CTQ2007-61690), the Centre National de la Recherche Scientifique (CNRS, France), and the European Union through the TMR program (Contract ERBFM-RXCT980181), the Network QuEMOLNA (Project MRTN-CT-2003-504880), and the Magmanet Network of Excellence (Contract 03/197). J. C. acknowledges the Universitat de València for a grant as invited researcher. We are specially thankful to our colleagues in the groups led by Prof. C. Ruiz-Pérez (Universidad de la Laguna, Spain) and Prof. H. O. Stumpf (Universidade Federal de Minas Gerais, Brazil), whose efforts have undoubtedly contribute to the advancement of the research on the metallosupramolecular chemistry of aromatic oligo-oxamato ligands. Thanks are also extended to Dr S. Stiriba and Prof. P. Amorós (Universitat de València, Spain) and Prof. J. C. Lacroix (Université Paris 7, France) for very stimulating talks and continuous interest in the work on molecular magnetic devices and multifunctional molecular magnets.

References

1 (*a*) E. C. Constable, *Prog. Inorg. Chem.*, 1994, **42**, 67; (*b*) J. M. Lehn, *Supramolecular Chemistry: Concepts and Perspectives*, VCH, Weinheim, Germany, 1995; (*c*) *Transition Metals in Supramolecular Chemistry*, ed. J. P. Sauvage, Wiley, New York, USA, 1999, vol. 5.
2 (*a*) S. Lenninger, B. Olenyuk and J. Stang, *Chem. Rev.*, 2000, **100**, 853; (*b*) G. F. Swiegers and T. J. Malefetse, *Chem. Rev.*, 2000, **100**, 3483; (*c*) P. J. Steel, *Acc. Chem. Res.*, 2005, **38**, 243.
3 (*a*) P. J. Stang and B. Olenyuk, *Acc. Chem. Res.*, 1997, **30**, 502; (*b*) S. R. Seidel and P. J. Stang, *Acc. Chem. Res.*, 2002, **35**, 972.
4 (*a*) M. Fujita, *Chem. Soc. Rev.*, 1998, **27**, 417; (*b*) M. Fujita, *Acc. Chem. Res.*, 1999, **32**, 53; (*c*) M. Fujita, M. Tominaga, A. Hori and B. Therrien, *Acc. Chem. Res.*, 2005, **38**, 369.
5 R. V. Slone, K. D. Beenkstein, S. Bélanger, J. T. Hupp, I. A. Guzei and A. L. Reinghold, *Coord. Chem. Rev.*, 1998, **171**, 221.
6 (*a*) F. Würthner, C. C. You and C. R. Saha-Möller, *Chem. Soc. Rev.*, 2004, **33**, 133; (*b*) F. Würthner, *Chem. Commun.*, 2004, 1564.
7 R. Ziessel, *Coord. Chem. Rev.*, 2001, **216–217**, 195.
8 (*a*) M. Albrecht, *Chem. Soc. Rev.*, 1998, **27**, 281; (*b*) C. A. Schalley, A. Lützen and M. Albrecht, *Chem.–Eur. J.*, 2004, **10**, 1072; (*c*) M. Albrecht, I. Janser and R. Fröhlich, *Chem. Commun.*, 2005, 157.
9 (*a*) D. L. Caulder and K. N. Raymond, *Acc. Chem. Res.*, 1999, **32**, 975; (*b*) D. L. Caulder and K. N. Raymond, *J. Chem. Soc., Dalton Trans.*, 1999, 1185; (*c*) D. Fiedler, D. H. Leung, R. G. Bergman and K. N. Raymond, *Acc. Chem. Res.*, 2005, **38**, 351.
10 L. K. Thompson, *Coord. Chem. Rev.*, 2002, **233–234**, 193.
11 (*a*) J. M. Lehn, *Angew. Chem., Int. Ed.*, 2004, **43**, 3644; (*b*) M. Ruben, J. M. Lehn and P. Müller, *Chem. Soc. Rev.*, 2006, **35**, 1056.
12 (*a*) O. Kahn, *Molecular Magnetism*, VCH, New York, USA, 1993; (*b*) *Magnetism: A Supramolecular Function*, ed. O. Kahn, NATO ASI Series C, Kluwer, Dordrecht, Germany, 1996, vol. 484.
13 M. Pilkington and S. Decurtins, in *Comprehensive Coordination Chemistry II: From Biology to Nanotechnology*, ed. J. A. McCleverty and T. J. Meyer, Elsevier, Oxford, 2004, vol. 7, p. 177.
14 (*a*) M. Verdaguer, A. Bleuzen, V. Marvaud, J. Vaissermann, M. Seuleiman, C. Desplanches, A. Scuiller, C. Train, R. Garde, G. Gelly, C. Lomenech, I. Rosenman, P. Veillet, C. Cartier and F. Villain, *Coord. Chem. Rev.*, 1999, **190–192**, 1023; (*b*) V. Marvaud, J. M. Herrera, T. Barilero, F. Tuyèras, R. Garde, A. Scuiller, C. Decroix, M. Cantuel and C. Desplanches, *Monatsh. Chem.*, 2003, **134**, 149; (*c*) R. Lescouëzec, L. M. Toma, J. Vaissermann, M. Verdaguer, F. S. Delgado, C. Ruiz-Pérez, F. Lloret and M. Julve, *Coord. Chem. Rev.*, 2005, **249**, 2691.
15 M. Ohba and H. Okawa, *Coord. Chem. Rev.*, 2000, **198**, 313.
16 L. M. C. Beltran and J. R. Long, *Acc. Chem. Res.*, 2005, **38**, 325.
17 (*a*) S. Decurtins, R. Pellaux, G. Antorrena and F. Palacio, *Coord. Chem. Rev.*, 1999, **190–192**, 841; (*b*) M. Pilkington, M. Gross, P. Franz, M. Biner, S. Decurtins, H. Stoeckli-Evans and A. Neels, *J. Solid State Chem.*, 2001, **159**, 262.
18 (*a*) E. Coronado, M. Clemente-León, J. R. Galán-Mascaros, C. Giménez-Saiz, C. J. Gómez-García and E. Martínez-Ferrero, *J. Chem. Soc., Dalton Trans.*, 2000, 3955; (*b*) E. Coronado, A. Forment-Aliaga, J. R. Galán-Mascaros, C. Giménez-Saiz, C. J. Gómez-García, E. Martínez-Ferrero, A. Nuez and F. M. Romero, *Solid State Sci.*, 2003, **5**, 917; (*c*) E. Coronado and J. R. Galán-Mascaros, *J. Mater. Chem.*, 2005, **15**, 66.
19 M. Gruselle, C. Train, K. Boubekeur, P. Gredin and N. Ovanesyan, *Coord. Chem. Rev.*, 2006, **250**, 2491.
20 (*a*) D. Gatteschi, R. Sessoli and J. Villain, *Molecular Nanomagnets*, Oxford University Press, UK, 2006; (*b*) D. Gatteschi and R. Sessoli, *Angew. Chem., Int. Ed.*, 2003, **42**, 268.
21 (*a*) C. Coulon, H. Miyasaka and R. Clérac, *Struct. Bonding*, 2006, **122**, 163; (*b*) H. Miyasaka and M. Yamashita, *Dalton Trans.*, 2007, 399.
22 (*a*) W. Linert and M. Verdaguer, *Molecular Magnets. Recent Highlights*, Springer Verlag, 2003; (*b*) O. Kahn, *Adv. Inorg. Chem.*, 1995, **43**, 179; (*c*) J. S. Miller and A. J. Epstein, *Angew. Chem., Int. Ed. Engl.*, 1994, **33**, 385.
23 (*a*) O. Kahn, *Struct. Bonding*, 1987, **68**, 89; (*b*) O. Kahn, *Acc. Chem. Res.*, 2000, **33**, 647.
24 (*a*) B. Cervera, J. L. Sanz, M. J. Ibañez, G. Vila, F. Lloret, M. Julve, R. Ruiz, X. Ottenwaelder, A. Aukauloo, S. Poussereau, Y. Journaux and M. C. Muñoz, *J. Chem. Soc., Dalton Trans.*, 1998, 781; (*b*) A. Aukauloo, X. Ottenwaelder, R. Ruiz, Y. Journaux, Y. Pei, E. Rivière, B. Cervera and M. C. Muñoz, *Eur. J. Inorg. Chem.*, 1999, 209; (*c*) A. Aukauloo, X. Ottenwaelder, R. Ruiz, S. Poussereau, Y. Pei, Y. Journaux, P. Fleurat, F. Volatron, B. Cervera and M. C. Muñoz, *Eur. J. Inorg. Chem.*, 1999, 1067; (*d*) K. E. Berg, Y. Pellegrin, G. Blondin, X. Ottenwaelder, Y. Journaux, M. M. Canovas, T. Mallah, S. Parsons and A. Aukauloo, *Eur. J. Inorg. Chem.*, 2002, 323; (*e*) X. Ottenwaelder, R. Ruiz-García, G. Blondin, R. Carrasco, J. Cano, D. Lexa, Y. Journaux and A. Aukauloo, *Chem. Commun.*, 2004, 504.
25 (*a*) Y. Pei, Y. Journaux, A. Dei, O. Kahn and D. Gatteschi, *J. Chem. Soc., Chem. Commun.*, 1986, 1300; (*b*) Y. Pei, Y. Journaux and O. Kahn, *Inorg. Chem.*, 1988, **27**, 399; (*c*) J. Ribas, C. Díaz, R. Costa, Y. Journaux, C. Mathonière, O. Kahn and A. Gleizes, *Inorg. Chem.*, 1990, **29**, 2042; (*d*) R. Vicente, A. Escuer and J. Ribas, *Polyhedron*, 1992, **11**, 857; (*e*) R. Costa, A. García, J. Ribas, T. Mallah, Y. Journaux, J. Sletten and X. Solans, *Inorg. Chem.*, 1993, **32**, 3733; (*f*) J. Ribas, C. Diaz, X. Solans and M. Font-Bardia, *Inorg. Chim. Acta*, 1995, **231**, 229; (*g*) M. Fettouhi, L. Ouahab, A. Boukhari, O. Cador, C. Mathonière and O. Kahn, *Inorg. Chem.*, 1996, **35**, 4932; (*h*) J. Ribas, C. Diaz, X. Solans and M. Font-Bardia, *J. Chem. Soc., Dalton Trans.*, 1997, 35; (*i*) M. M. Miao, P. Cheng, D. Z. Liao, Z. H. Jiang and G. L. Wang, *Transition Met. Chem.*, 1997, **22**, 19; (*j*) M. M. Miao, P. Cheng, D. Z. Liao, Z. H. Jiang and G. L. Wang, *Transition Met. Chem.*, 1997, **22**, 330; (*k*) A. Aukauloo, X. Ottenwaelder, R. Ruiz, Y. Journaux, Y. Pei, E. Rivière and M. C. Muñoz, *Eur. J. Inorg. Chem.*, 2000, 951; (*l*) E. Q. Gao, Q. H. Zhao, J. K. Tang, D. Z. Liao, Z. H. Jiang and S. P. Yan, *J. Chem. Soc., Dalton Trans.*, 2001, 1537; (*m*) J. Tercero, C. Diaz, M. S. El Fallah, J. Ribas, X. Solans, M. A. Maestro and J. Mahía, *Inorg. Chem.*, 2001, **40**, 3077; (*n*) E. Q. Gao, J. K. Tang, D. Z. Liao, Z. H. Jiang, S. P. Yan and G. L. Wang, *Inorg. Chem.*, 2001, **40**, 3134; (*o*) J. Tercero, C. Diaz, J.

Ribas, J. Mahía and M. A. Maestro, *Inorg. Chem.*, 2002, **41**, 5373; (*p*) J. Tercero, C. Diaz, J. Ribas, J. Mahía, M. A. Maestro and X. Solans, *J. Chem. Soc., Dalton Trans.*, 2002, 2040; (*q*) J. Tercero, C. Diaz, J. Ribas, X. Solans, M. Maestro, J. Mahía and H. Stoeckli-Evans, *Inorg. Chem.*, 2003, **42**, 3366; (*r*) T. Rüffer, B. Bräuer, A. K. Powell, I. Hewitt and G. Salvan, *Inorg.Chim. Acta*, 2007, **360**, 3475.

26 (*a*) Y. Pei, M. Verdaguer, O. Kahn, J. Sletten and J. P. Renard, *J. Am. Chem. Soc.*, 1986, **108**, 7428; (*b*) Y. Pei, M. Verdaguer, O. Kahn, J. Sletten and J. P. Renard, *Inorg. Chem.*, 1987, **26**, 138; (*c*) O. Kahn, Y. Pei, M. Verdaguer, J. P. Renard and J. Sletten, *J. Am. Chem. Soc.*, 1988, **110**, 782; (*d*) P. J. Van Kroningsbruggen, O. Kahn, K. Nakatani, Y. Pei, J. P. Renard, M. Drillon and P. Legoll, *Inorg. Chem.*, 1990, **29**, 3325; (*e*) K. Nakatani, P. Bergerat, E. Codjovi, C. Mathonière, Y. Pei and O. Kahn, *Inorg. Chem.*, 1991, **30**, 3977; (*f*) H. O. Stumpf, Y. Pei, L. Ouahab, F. Leberre, E. Codjovi and O. Kahn, *Inorg. Chem.*, 1993, **32**, 5687; (*g*) V. Baron, B. Gillon, J. Sletten, C. Mathonière, E. Codjovi and O. Kahn, *Inorg. Chim. Acta*, 1995, **235**, 69; (*h*) S. Tunner, O. Kahn and L. Rabardel, *J. Am. Chem. Soc.*, 1996, **118**, 6428; (*i*) V. Baron, B. Gillon, A. Cousson, C. Mathonière, O. Kahn, A. Grand, L. Öhrström, B. Delley, M. Bonnet and J. X. Boucherle, *J. Am. Chem. Soc.*, 1997, **119**, 3500; (*j*) O. Cador, C. Mathonière and O. Kahn, *Inorg. Chem.*, 2000, **39**, 3799; (*k*) L. C. Meira-Belo, U. A. Litao, C. L. M. Pereira, A. Doriguetto, N. G. Fernandes and H. O. Stumpf, *J. Magn. Magn. Mater.*, 2001, **226–230**, 2018; (*l*) H. O. Stumpf, C. L. M. Pereira, A. C. Doriguetto, C. Konzen, L. C. B. Meira, N. G. Fernandes, Y. P. Mascarenhas, J. Ellena and M. Knobel, *Eur. J. Inorg. Chem.*, 2005, **24**, 5018.

27 (*a*) H. O. Stumpf, Y. Pei, O. Kahn, J. Sletten and J. P. Renard, *J. Am. Chem. Soc.*, 1993, **115**, 6738; (*b*) H. O. Stumpf, L. Ouahab, Y. Pei, D. Grandjean and O. Kahn, *Science*, 1993, **261**, 447; (*c*) H. O. Stumpf, L. Ouahab, Y. Pei, P. Bergerat and O. Kahn, *J. Am. Chem. Soc.*, 1994, **116**, 3866; (*d*) H. O. Stumpf, Y. Pei, C. Michaut, O. Kahn, J. P. Renard and L. Ouahab, *Chem. Mater.*, 1994, **6**, 257; (*e*) O. Cador, D. Price, J. Larianova, C. Mathonière, O. Kahn and J. V. Yakhmi, *J. Mater. Chem.*, 1997, **7**, 1263; (*f*) R. M. Kadam, M. D. Sastry, M. K. Bhide, S. A. Chavan, J. V. Yakhmi and O. Kahn, *Chem. Phys. Lett.*, 1997, **281**, 292; (*g*) M. G. F. Vaz, L. M. M. Pinheiro, H. O. Stumpf, A. F. C. Alcantara, S. Golhen, L. Ouahab, O. Cador, C. Mathonière and O. Kahn, *Chem.–Eur. J.*, 1999, **5**, 1486; (*h*) O. Cador, M. G. F. Vaz, H. O. Stumpf, C. Mathonière and O. Kahn, *Synth. Met.*, 2001, **122**, 559; (*i*) M. G. F. Vaz, E. F. Pedroso, N. L. Speziali, M. A. Novak, A. F. C. Alcantara and H. O. Stumpf, *Inorg. Chim. Acta*, 2001, **326**, 65; (*j*) M. C. Dias, M. Knobel and H. O. Stumpf, *J. Magn. Magn. Mater.*, 2001, **226–230**, 1961; (*k*) M. G. F. Vaz, J. D. Ardisson, H. O. Stumpf and W. A. A. Macedo, *J. Magn. Magn. Mater.*, 2001, **226–230**, 2028; (*l*) R. M. Kadam, M. K. Bhide, M. D. Sastry, J. V. Yakhmi and O. Kahn, *Chem. Phys. Lett.*, 2002, **357**, 457; (*m*) M. G. F. Vaz, J. D. Ardisson, N. L. Speziali, G. P. Souza, H. O. Stumpf, M. Knobel and W. A. A. Macedo, *Polyhedron*, 2001, **20**, 1431; (*n*) C. L. M. Pereira, E. F. Pedroso, M. A. Novak, A. L. Brandl, M. Knobel and H. O. Stumpf, *Polyhedron*, 2003, **22**, 2387; (*o*) M. A. Novak, M. G. F. Vaz, N. L. Speziali, W. V. Costa and H. O. Stumpf, *Polyhedron*, 2003, **22**, 2391.

28 (*a*) X. Ottenwaelder, Ph. D. Thesis, University of Paris-Sud, 2001; (*b*) E. Pardo, Ph. D. Thesis, University of València, 2006; (*c*) Y. Filali, Ph. D. Thesis, University Pierre et Marie Curie, 2007.

29 (*a*) E. Pardo, R. Ruiz-García, F. Lloret, J. Faus, M. Julve, Y. Journaux, F. S. Delgado and C. Ruiz-Pérez, *Adv. Mater.*, 2004, **16**, 1597; (*b*) E. Pardo, R. Ruiz-García, F. Lloret, J. Faus, M. Julve, Y. Journaux, M. A. Novak, F. S. Delgado and C. Ruiz-Pérez, *Chem.–Eur. J.*, 2007, **13**, 2054.

30 (*a*) I. Fernández, R. Ruiz, J. Faus, M. Julve, F. Lloret, J. Cano, X. Ottenwaelder, Y. Journaux and M. C. Muñoz, *Angew. Chem., Int. Ed.*, 2001, **40**, 3039; (*b*) E. Pardo, J. Faus, M. Julve, F. Lloret, M. C. Muñoz, J. Cano, X. Ottenwaelder, Y. Journaux, R. Carrasco, G. Blay, I. Fernández and R. Ruiz-García, *J. Am. Chem. Soc.*, 2003, **125**, 10770; (*c*) E. Pardo, R. Carrasco, R. Ruiz-García, M. Julve, F. Lloret, M. C. Muñoz, Y. Journaux, E. Ruiz and J. Cano, *J. Am. Chem. Soc.*, 2008, **130**, 576.

31 E. Pardo, D. Cangussu, M. C. Dul, R. Lezcouëzec, Y. Journaux, L. M. Chamoreau, J. Pasán, C. Ruiz-Pérez, R. Carrasco, J. Cano, M. Julve, F. Lloret and R. Ruiz-García, manuscript in preparation.

32 (*a*) E. Pardo, K. Bernot, F. Lloret, M. Julve, R. Ruiz-García, J. Pasán, C. Ruiz-Pérez, D. Cangussu, V. Costa, R. Lescouëzec and Y. Journaux, *Eur. J. Inorg. Chem.*, 2007, 4569; (*b*) E. Pardo, R. Ruiz-García, F. Lloret, M. Julve, F. Delgado, C. Ruiz-Pérez, D. Cangussu, V. Costa, R. Lescouëzec and Y. Journaux, manuscript in preparation.

33 (*a*) E. Pardo, K. Bernot, M. Julve, F. Lloret, J. Cano, R. Ruiz-García, F. S. Delgado, C. Ruiz-Pérez, X. Ottenwaelder and Y. Journaux, *Inorg. Chem.*, 2004, **43**, 2768; (*b*) E. Pardo, R. Ruiz-García, F. Lloret, M. Julve, J. Cano, J. Pasán, C. Ruiz-Pérez, Y. Filali, L. M. Chamoreau and Y. Journaux, *Inorg. Chem.*, 2007, **46**, 4504.

34 (*a*) E. Pardo, K. Bernot, M. Julve, F. Lloret, J. Cano, R. Ruiz-García, J. Pasán, C. Ruiz-Pérez, X. Ottenwaelder and Y. Journaux, *Chem. Commun.*, 2004, 920; (*b*) E. Pardo, I. Morales-Osorio, M. Julve, F. Lloret, J. Cano, R. Ruiz-García, J. Pasán, C. Ruiz-Pérez, X. Ottenwaelder and Y. Journaux, *Inorg. Chem.*, 2004, **43**, 7594; (*c*) E. Pardo, P. Burguete, R. Ruiz-García, M. Julve, D. Beltrán, Y. Journaux, P. Amorós and F. Lloret, *J. Mater. Chem.*, 2006, **16**, 2702; (*d*) E. Pardo, R. Ruiz-García, F. Lloret, M. Julve, J. Cano, J. Pasán, C. Ruiz-Pérez, M.-C. Dul, R. Lescouëzec, L.-M. Chamoreau and Y. Journaux, manuscript in preparation.

35 C. L. M. Pereira, E. Pedroso, H. O. Stumpf, M. A. Novak, L. Ricard, R. Ruiz-García, E. Rivière and Y. Journaux, *Angew. Chem., Int. Ed.*, 2004, **43**, 955.

36 (*a*) D. Cangussu, E. Pardo, M.-C. Dul, R. Lescouëzec, P. Herson, Y. Journaux, E. F. Pedroso, C. L. M. Pereira, H. O. Stumpf, M. C. Muñoz, R. Ruiz-García, J. Cano, M. Julve and F. Lloret, *Inorg. Chim. Acta*, 2008, DOI: 10.1016/j.ica.2008.02.042; (*b*) E. Pardo, D. Cangassu, M.-C. Dul, R. Lescouëzec, P. Herson, Y. Journaux, E. F. Pedroso, C. L. M. Pereira, M. C. Muñoz, R. Ruiz-García, J. Cano, P. Amorós, M. Julve and F. Lloret, *Angew. Chem., Int. Ed.*, in press.

37 (*a*) X. Ottenwaelder, J. Cano, Y. Journaux, E. Rivière, C. Brennan, M. Nierlich and R. Ruiz-García, *Angew. Chem., Int. Ed.*, 2004, **43**, 850; (*b*) M. C. Dul, E. Pardo, R. Lezcouëzec, Y. Journaux, L. M. Chamoreau, J. Cano, M. Julve, F. Lloret and R. Ruiz-García, manuscript in preparation.

38 (*a*) C. Piguet, G. Bernardinelli and G. Hopfgartner, *Chem. Rev.*, 1997, **97**, 2005; (*b*) A. Williams, *Chem.–Eur. J.*, 1997, **3**, 15; (*c*) M. Albrecht, *Chem.–Eur. J.*, 2000, **6**, 3485; (*d*) M. Albrecht, *Chem. Rev.*, 2001, **101**, 3457.

39 (*a*) J. A. McCleverty and M. D. Ward, *Acc. Chem. Res.*, 1998, **36**, 3447; (*b*) T. Glaser, M. Gerenkamp and R. Fröhlich, *Angew. Chem., Int. Ed.*, 2002, **41**, 3823; (*c*) T. Glaser, M. Heidemeier, J. B. H. Strautmann, H. Bögge, A. Stammler, E. Krickemeyer, R. Huenerbein, S. Grimme, E. Bothe and E. Bill, *Chem.–Eur. J.*, 2007, **13**, 9191.

40 (*a*) D. A. Dougherty, *Acc. Chem. Res.*, 1991, **24**, 88; (*b*) H. Iwamura and N. Koga, *Acc. Chem. Res.*, 1993, **26**, 346; (*c*) S. J. Jacobs, D. A. Shultz, R. Jain, J. Novak and D. A. Dougherty, *J. Am. Chem. Soc.*, 1993, **115**, 1744; (*d*) N. Nakamura, K. Inoue and H. Iwamura, *Angew. Chem., Int. Ed. Engl.*, 1993, **32**, 872; (*e*) A. Rajca, *Chem. Rev.*, 1994, **94**, 871.

41 (*a*) A. Caneschi, A. Dei, H. Lee, D. A. Shultz and L. Sorace, *Inorg. Chem.*, 2001, **40**, 408; (*b*) A. Caneschi, A. Dei, C. P. Mussari, D. A. Shultz, L. Sorace and K. E. Vostrikova, *Inorg. Chem.*, 2002, **41**, 1086.

42 (*a*) J. A. Mydosh, *Spin Glasses: An Experimental Introduction*, Taylor & Francis, London, UK, 1993; (*b*) D. Chowdhury, *Spin Glasses and Other Frustrated Systems*, Princeton University Press, New Jersey, USA, 1986.

43 (*a*) M. Eddaoudi, D. M. Moler, H. Li, B. Chen, T. M. Reineke, M. O'Keeffe and O. M. Yaghi, *Acc. Chem. Res.*, 2001, **34**, 319; (*b*) O. M. Yaghi, M. O'Keeffe, N. W. Ockwig, H. K. Chae, M. Eddaoudi and J. Kim, *Nature*, 2003, **423**, 705.

44 (*a*) E. Clar, *Polycyclic Hydrocarbons*, Academic Press, London, UK, 1964, vol. 1 and 2; (*b*) Y. Geerts, G. Klärner and K. Müllen, in *Electronic Materials: The Oligomer Approach*, ed. K. Müllen and G. Klärner, Wiley-VCH, Weinheim, Germany, 1998, p. 48.

45 M. Irie, *Chem. Rev.*, 2000, **100**, 1685.

46 (*a*) Y. Nakamura and H. Iwamura, *Bull. Chem. Soc. Jpn.*, 1993, **66**, 3724; (*b*) M. M. Wienk and R. A. J. Janssen, *J. Am. Chem. Soc.*, 1996, **118**, 10625; (*c*) M. M. Wienk and R. A. J. Janssen, *J. Am. Chem. Soc.*, 1997, **119**, 4492.

47 (*a*) *Molecular Electronics*, ed. J. Jorner and M. Ratner, M., Blackwell Science, Oxford, USA, 1997; (*b*) *Molecular Electronics: Science and Technology*, ed. A. Aviram and M. Ratner, Annals of the New York Academy of Sciences, New York, USA, 1998; (*c*) B. L. Feringa, *MolecularSwitches*, VCH, New York, USA, 2001; (*d*) V. Balzani and M. Venturi, *Molecular Machines and Devices*, Wiley-VCH, Weinheim, Germany, 2003; (*e*) V. Balzani, A. Credi and M. Venturi, *Chem.–Eur. J.*, 2002, **8**, 5524.

48 (*a*) V. Balzani, A. Credi and M. Venturi, *Coord. Chem. Rev.*, 1998, **171**, 2; (*b*) A. J. Vlcek, *Electron Transfer in Chemistry*, Wiley-VCH, Weinheim, Germany, 2001, p. 804.
49 (*a*) *Spin Crossover in Transition Metal Compounds*, ed. P. Gütlich and H. A. Godwin, Springer, Berlin, Germany, 2004, vol. 233–235; (*b*) J. A. Real, A. B. Gaspar and M. C. Muñoz, *Dalton Trans.*, 2005, 2062.
50 (*a*) J. L. Serrano, *Metallomesogens*, VCH, Weinheim, Germany, 1996; (*b*) S. J. Rowan, *Angew. Chem., Int. Ed.*, 2005, **44**, 4830.
51 Thematic issues on nanoscopic functional materials and molecular magnetic materials: (*a*) *Chem. Mater.*, 2001, **13**, 3059; (*b*) *Chem. Rev.*, 2005, **105**, 1023; (*c*) *J. Mater. Chem.*, 2006, **16**, 2513.
52 (*a*) A. P. Alivisatos, P. F. Barbara, A. W. Castleman, J. Chang, D. A. Dixon, M. L. Klein, G. L. McLendon, J. S. Miller, M. A. Ratner, P. J. Rossky, S. I. Stupp and M. E. Thompson, *Adv. Mater.*, 1998, **10**, 1297; (*b*) E. Dujardin and S. Mann, *Adv. Mater.*, 2004, **16**, 112.